

Grounding Language in Play

Corey Lynch* Pierre Sermanet*
Robotics at Google¹

Abstract

Natural language is perhaps the most versatile and intuitive way for humans to communicate tasks to a robot. Prior work on **Learning from Play** (LfP) (Lynch et al., 2019) provides a simple approach for learning a wide variety of robotic behaviors from general sensors. However, each task must be specified with a goal image—something that is not practical in open-world environments. In this work we present a simple and scalable way to condition policies on human language instead. We extend LfP by pairing short robot experiences from play with relevant human language after-the-fact. To make this efficient, we introduce *multi-context imitation*, which allows us to train a single agent to follow image or language goals, then use just language conditioning at test time. This reduces the cost of language pairing to less than 1% of collected robot experience, with the majority of control still learned via self-supervised imitation. At test time, a single agent trained in this manner can perform many different robotic manipulation skills in a row in a 3D environment,

directly from images, and specified only with natural language (e.g. “open the drawer...now pick up the block...now press the green button...”) (video). Finally, we introduce a simple technique that transfers knowledge from large unlabeled text corpora to robotic learning. We find that transfer significantly improves downstream robotic manipulation. It also allows our agent to follow thousands of novel instructions at test time in zero shot, in 16 different languages. See videos of our experiments at language-play.github.io

1. Introduction

A long-term motivation in robotic learning is the idea of a generalist robot—a single agent that can solve many tasks in everyday settings, using only general onboard sensors. A fundamental but less considered aspect, alongside task and observation space generality, is *general task specification*: the ability for untrained users to direct agent behavior using

* Equal contribution ¹g.co/robotics. {coreylynch,sermanet}@google.com

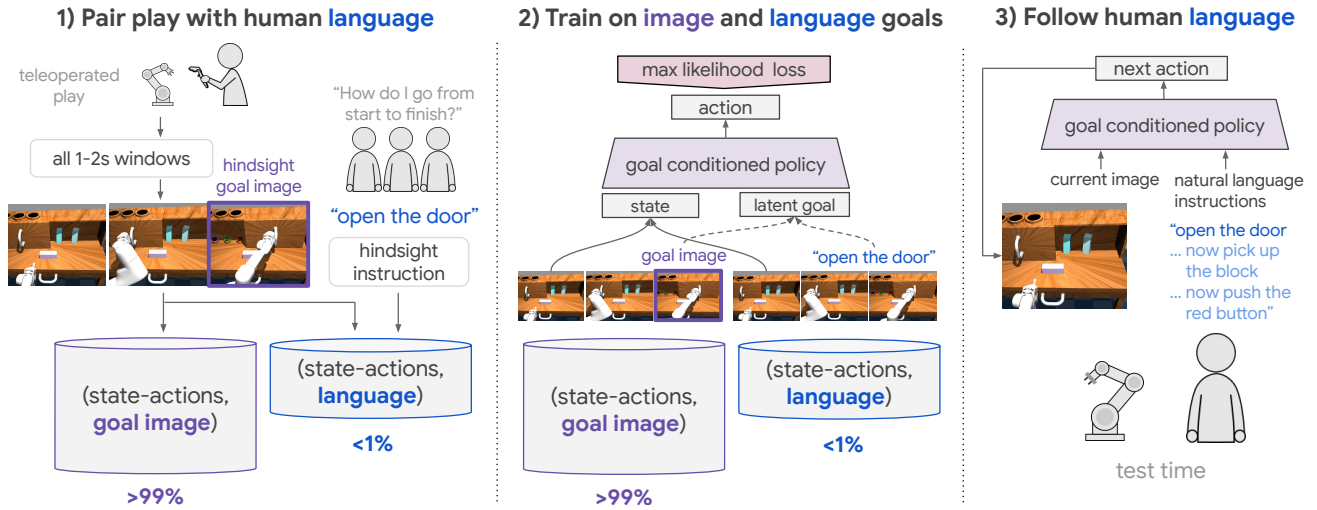


Figure 1: **Learning to follow human language instructions from play.** 1) First, relabel teleoperated play into many image goal examples. Next, pair a small amount of play with hindsight instructions, yielding language goal examples. 2) Multicontext imitation: train a single policy on both image and language goals. 3) Test time: A single agent performs many skills in a row, directly from images, specified only in natural language.

the most intuitive and flexible mechanisms. Along these lines, it is hard to imagine a truly generalist robot without also imagining a robot that can follow instructions expressed in natural language.

More broadly, children learn language in the context of a rich, relevant, sensorimotor experience (Sachs et al., 1981; Smith and Gasser, 2005). This motivates the long-standing question in artificial intelligence of *embodied language acquisition* (Harnad, 1990; Mooney, 2008): how might intelligent agents ground language understanding in their own embodied perception? An ability to relate language to the physical world potentially allows robots and humans to communicate on common ground over shared sensory experience (Clark and Brennan, 1991; Bisk et al., 2020) — something that could lead to much more meaningful forms of human-machine interaction.

Furthermore, language acquisition, at least in humans, is a highly *social* process (Skinner, 1957; Baldwin and Meyer, 2007; Verga and Kotz, 2013). During their earliest interactions, infants contribute actions while caregivers contribute relevant words (Clark and Brennan, 1991). While we cannot speculate on the actual learning mechanism at play in humans, we are interested in what robots can learn from similar paired data. In this work, we ask: assuming real humans play a critical role in robot language acquisition, what is the most efficient way to go about it? How can we scalably pair robot experience with relevant human language to bootstrap instruction following?

Even simple instruction following, however, poses a notoriously difficult learning challenge, subsuming many long-term problems in AI (Hermann et al., 2017; Das et al., 2018). For example, a robot presented with the command “sweep the block into the drawer must be able to relate language to low-level perception (what does a block look like? what is a drawer?). It must perform visual reasoning (what does it mean for the block to be in the drawer?). Finally, it must solve a complex sequential decision problem (what commands do I send to my arm to “sweep”?). We note these questions cover only a single task, whereas the generalist robot setting demands single agents that perform many.

In this work, we combine the setting of open-ended robotic manipulation with open-ended human language conditioning. There is a long history of work studying instruction following (survey (Luketina et al., 2019)). Prior work typically studies restricted observation spaces (e.g. games (Goyal et al., 2019), 2D gridworlds (Yu et al., 2018)), simplified actuators, (e.g. binary pick and place primitives (Hill et al., 2019)), and synthetic language data (Hermann et al., 2017). We study the first combination, to our knowledge, of 1) human language instructions, 2) high-dimensional continuous sensory inputs and actuators, and 3) complex tasks like long-horizon robotic object manipulation. The test time scenario

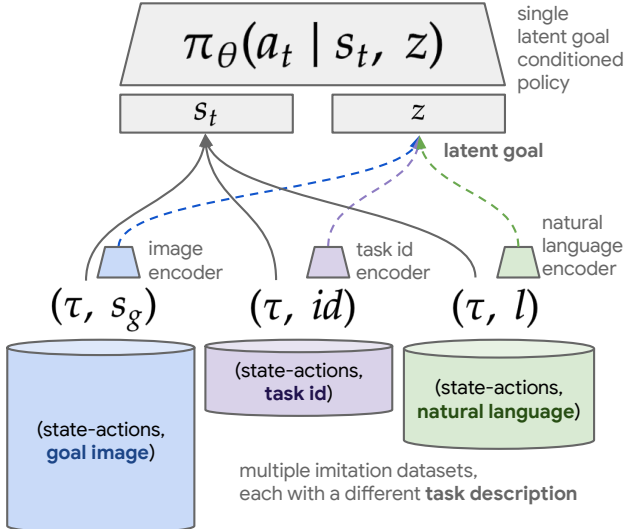


Figure 2: **Multicontext Imitation Learning.** We introduce Multicontext Imitation Learning (MCIL), a simple generalization of contextual imitation learning to multiple heterogeneous contexts. An increasingly typical scenario in imitation learning is one where we have *multiple* imitation datasets, each with a different task description (e.g. goal image, task id, natural language, video demonstration, etc.) and different cost of collection. MCIL trains 1) a single *latent goal* conditioned policy over all datasets and 2) a set of encoders, one per dataset, each responsible for mapping a particular task description to the shared latent space.

we consider is a single agent that can perform many tasks in a row, each specified by a human in natural language. For example, “open the door all the way to the right...now pick up the block...now push the red button...now close the door”. Furthermore, the agent should be able to perform any combination of subtasks in any order. We refer to this as the “ask me anything” scenario (Fig. 1, step 3), which tests three important aspects of generality: general-purpose control, learning from onboard sensors, and general task specification.

Prior work on Learning from Play (LfP) (Lynch et al., 2019) provides a simple starting point for learning general-purpose skills from onboard sensors: first cover state space with teleoperated “play” data, then use relabeled imitation learning to distill many reusable behaviors into a goal-directed policy. However, like other methods that combine relabeling with image observations, (Warde-Farley et al., 2018; Nair et al., 2018; Pong et al., 2019; Nair et al., 2019; Florensa et al., 2019), LfP requires that tasks be specified using a goal image to reach. While trivial in a simulator, this form of task specification is often impractical in open-world environments.

In this work, we present a simple approach that extends LfP to the natural language conditioned setting. Fig. 1 provides an overview, which has four main steps:

1. **Cover the space with teleoperated play** (Fig. 1, step 1) Collect a teleoperated “play” dataset. These long temporal state-action logs are automatically relabeled into many short-horizon demonstrations, solving for image goals.
2. **Pair play with human language** (Fig. 1, step 1). Typical setups pair instructions with optimal behavior. Instead, we pair any behavior from play after-the-fact with optimal *instructions*, a process we call Hindsight Instruction Pairing. This collection method is the first contribution of this paper. It yields a dataset of demonstrations, solving for human language goals.
3. **Multicontext imitation learning** (Fig. 1, step 2): We train a single policy to solve image or language goals, then use only language conditioning at test time. To make this possible, we introduce Multicontext Imitation Learning (Fig. 2). This is the second contribution of this paper. This approach is highly data efficient. It reduces the cost of language pairing to less than 1% of collected robot experience to enable language conditioning, with the majority of control still learned via self-supervised imitation.
4. **Condition on human language at test time.** (Fig. 1, step 3) At test time, our experiments show that a single policy trained in this manner can perform many complex robotic manipulation skills in a row, directly from images, and specified entirely with natural language (see [video](#)).

Finally, we study **transfer learning from unlabeled text corpora to robotic manipulation**. We introduce a simple transfer learning augmentation, applicable to any language conditioned policy. We find that this significantly improves downstream robotic manipulation. This is the first instance, to our knowledge, of this kind of transfer. Importantly, this same technique allows our agent to follow thousands of novel instructions in zero shot, across 16 different languages. This is the third contribution of this work.

2. Related Work

Robotic learning from general sensors. In general, learning complex robotic skills from low-level sensors is possible, but requires substantial human supervision. Two of the most successful approaches are imitation learning (IL) (Atkeson and Schaal, 1997; Argall et al., 2009) and reinforcement learning (RL) (Kober et al., 2013; Levine et al., 2016; Kalashnikov et al., 2018; Haarnoja et al., 2018; Andrychowicz et al., 2020). IL typically requires many human demonstrations (Duan et al., 2017; Rajeswaran et al., 2017; Rahmatizadeh et al., 2018; Zhang et al., 2018) to drive supervised learning of a policy. In RL, supervision takes the

form of a well-shaped (Popov et al., 2017) hand-designed reward to drive autonomous trial and error learning. Designing reward functions in open-world environments is non-trivial, requiring either task-specific instrumentation (Gu et al., 2017) or learned perceptual rewards (Sermanet et al., 2017; 2018; Singh et al., 2019). Additionally, RL agents face difficult exploration problems (Thrun, 1992), often requiring hand-designed exploration strategies (Kalashnikov et al., 2018; Ebert et al., 2018) or even human demonstrations as well (Rajeswaran et al., 2017; Hester et al., 2018). Finally, conventional IL and RL only account for the training of a single task. Even under multitask formulations of RL (Teh et al., 2017) and IL (Rahmatizadeh et al., 2018), each new task considered requires a corresponding and sizable human effort. RL additionally faces significant optimization challenges (Schaul et al., 2019) in the multitask setting, often leading to worse data efficiency than learning tasks individually (Parisotto et al., 2015). This makes it difficult to scale either approach naively to the broad task setting of a generalist robot.

Task-agnostic control. This paper builds on the setting of task-agnostic control, where a single agent must be able to reach any reachable goal state in its environment upon command (Kaelbling, 1993; Schaul et al., 2015; Warde-Farley et al., 2018). One way of acquiring this kind of control is to first learn a model of the environment through interaction (Oh et al., 2015; Hafner et al., 2018; Ebert et al., 2018; Ha and Schmidhuber, 2018) then use it for planning. However, these approaches face the same intractable autonomous exploration problem that RL does, requiring either environments simple enough to explore fully with random actions or hand-scripted primitives to guide richer behavior. A powerful model-free strategy for task-agnostic control is goal relabeling (Kaelbling, 1993; Andrychowicz et al., 2017). This self-supervised technique trains goal conditioned policies to reach any previously visited state upon demand, with many recent examples in RL (Nair et al., 2018; Pong et al., 2018; Gupta et al., 2019; Pong et al., 2019; Ghosh et al., 2019; Eysenbach et al., 2020) and IL (Lynch et al., 2019; Ding et al., 2019). However, when combined high dimensional observation spaces like images, relabeling results in policies that must be instructed with goal images at test time—a prohibitively expensive assumption in open world (non-simulator) environments. The present work builds heavily on relabeled imitation, but additionally equips policies with flexible natural language conditioning.

Covering state space. Learning generally requires exposure to diverse training data. While relabeling allows for goal-directed learning from any experience, it cannot account for the *diversity* of that experience, which comes entirely from the underlying data. In task agnostic control, where agents must be prepared to reach any user-proposed goal state at test time, an effective data collection strategy

is one that visits as many states as possible during training (Pong et al., 2019). Obtaining this sort of state space coverage autonomously is a long-standing problem (Thrun, 1992) motivating work on tractable heuristics (Kolter and Ng, 2009), intrinsic motivation (Oudeyer et al., 2008; Schmidhuber, 2010), and more recent information-theoretic approaches (Pong et al., 2019; Lee et al., 2019). Success so far has been limited to restricted environments (Pathak et al., 2017), as automatic exploration quickly becomes intractable in complex settings like object manipulation, where even knowing which states are valid presents a major challenge (Pong et al., 2019). Teleoperated play data (Lynch et al., 2019) sidesteps this exploration problem entirely, using prior human knowledge of object affordances to cover state space. This type of data stands in contrast to conventional teleoperated multitask demonstrations (Zhang et al., 2018; Handa et al., 2019; Singh et al., 2020), whose diversity is necessarily constrained by an upfront task definition. Play data has served as the basis for relabeled IL (Lynch et al., 2019) and relabeled hierarchical RL (Gupta et al., 2019). Play combined with relabeled IL is a central component of this work.

Multicontext learning. A number of previous methods have focused on generalizing across tasks (Caruana, 1997), or generalizing across goals (Schaul et al., 2015). We introduce a framework for generalizing across heterogeneous task and goal *descriptions*, e.g. goal image and natural language. When one of the training sources is plentiful and the other scarce, multicontext learning can be seen as transfer learning (Tan et al., 2018) through a shared goal space. Multicontext imitation is a central component of our method, as it reduces the cost of human language supervision to the point where it can be practically applied to learn open-ended instruction following.

Instruction following. There is a long history of research into agents that not only learn a grounded language understanding (Winograd, 1972; Mooney, 2008), but demonstrate that understanding by following instructions (Luketina et al., 2019). Recently, authors have had success using deep learning to directly map raw input and text instructions to actions. However, prior work often studies restricted environments (MacMahon et al., 2006; Kollar et al., 2010; Andreas et al., 2016; Oh et al., 2017; Misra et al., 2017; Yu et al., 2017; 2018) and simplified actuators (Wang et al., 2019; Hill et al., 2019; Chaplot et al., 2018; Goyal et al., 2019; Shridhar et al., 2020). Additionally, learning to follow *natural* language is still not the standard in instruction-following research (Luketina et al., 2019), with typical implementations instead assuming access to simulator-provided instructions drawn from a restricted vocabulary and grammar (Hermann et al., 2017; Jiang et al., 2019). This work, in contrast, studies 1) natural language instructions, 2) high-dimensional continuous sensory inputs and actuators, and 3) complex tasks like

long-horizon 3D robotic object manipulation. Furthermore, unlike existing RL approaches to instruction following, our IL method is highly sample efficient, requires no reward definition, and trivially scales to the multitask setting.

Transfer learning from generic text corpora. Transfer learning from large “in the wild” text corpora, e.g. Wikipedia, to downstream tasks is prevalent in NLP (Devlin et al., 2018; Howard and Ruder, 2018; Radford et al., 2019; Raffel et al., 2019; Goldberg, 2019; Tenney et al., 2019), but has been relatively unexplored for language-guided control. An identified reason for this gap (Luketina et al., 2019) is that tasks studied so far use small synthetic language corpora and are typically too artificial to benefit from transfer from real-world textual corpora. Like (Shridhar et al., 2020), we study instruction following in a simulated 3D home with real-world semantics, but expand the setting further to robotic object manipulation under realistic physics. This allows us to show the first example, to our knowledge, of positive transfer from “in the wild” text corpora to instruction following, making our agent better at language-guided manipulation and allowing it to follow many instructions outside its training set.

3. Preliminaries

We first review the prior settings of relabeled imitation learning and LfP, then introduce LangLfP, our natural language extension of LfP which builds on these components.

3.1. Relabeled imitation learning

Goal conditioned learning (Kaelbling, 1993) trains a single agent to reach any goal. This is formalized as a goal conditioned policy $\pi_\theta(a|s, g)$, which outputs next action $a \in A$, conditioned on current state $s \in S$ and a task descriptor $g \in G$. Imitation approaches learn this mapping using supervised learning over a dataset $\mathcal{D} = \{(\tau, g)_i\}_i^N$, of expert state-action trajectories $\tau = \{(s_0, a_0), \dots\}$ solving for a paired task descriptor (typically a one-hot task encoding (Rahmatizadeh et al., 2018)). A convenient choice for a task descriptor is some goal state $g = s_g \in S$ to reach. This allows any state visited during collection to be *relabelled* (Kaelbling, 1993; Andrychowicz et al., 2017) as a “reached goal state”, with the preceding states and actions treated as optimal behavior for reaching that goal. Applied to some original dataset \mathcal{D} , this yields a much larger dataset of relabeled examples $\mathcal{D}_R = \{(\tau, s_g)_i\}_i^{N_R}$, $N_R \gg N$, providing the inputs to a simple maximum likelihood objective for goal directed control: relabeled goal conditioned behavioral cloning (GCBC) (Lynch et al., 2019; Ding et al., 2019):

$$\mathcal{L}_{\text{GCBC}} = \mathbb{E}_{(\tau, s_g) \sim \mathcal{D}_R} \left[\sum_{t=0}^{|\tau|} \log \pi_{\theta}(a_t | s_t, s_g) \right] \quad (1)$$

While relabeling automatically generates a large number of goal-directed demonstrations at training time, it cannot account for the *diversity* of those demonstrations, which comes entirely from the underlying data. To be able to reach *any* user-provided goal, this motivates data collection methods, upstream of relabeling, that fully cover state space.

3.2. Teleoperated play

Human teleoperated “play” collection (Lynch et al., 2019) directly addresses the state space coverage problem. In this setting, an operator is no longer constrained to a set of predefined tasks, but rather engages in every available object manipulation in a scene (example of play data). The motivation is to fully cover state space using prior human knowledge of object affordances. During collection, the stream of onboard robot observations and actions are recorded, $\{(s_t, a_t)\}_{t=0}^{\infty}$, yielding an unsegmented dataset of unstructured but semantically meaningful behaviors, useful in a relabeled imitation learning context.

3.3. Learning from play

LfP (Lynch et al., 2019) combines relabeled imitation learning with teleoperated play. First, unsegmented play logs are relabeled using Algorithm 2. This yields a training set $D_{\text{play}} = \{(\tau, s_g)_i\}_{i=0}^{D_{\text{play}}}$, holding many diverse, short-horizon examples. These can be fed to a standard maximum likelihood goal conditioned imitation objective:

$$\mathcal{L}_{\text{LfP}} = \mathbb{E}_{(\tau, s_g) \sim D_{\text{play}}} \left[\sum_{t=0}^{|\tau|} \log \pi_{\theta}(a_t | s_t, s_g) \right] \quad (2)$$

4. Learning Human Language Conditioned Control from Play

A limitation of LfP—and other approaches that combine relabeling with image state spaces—is that behavior must be conditioned on a goal image s_g at test time. In this work, we focus on a more flexible mode of conditioning: humans describing tasks in natural language. Succeeding at this requires solving a complicated grounding problem. To address this, we introduce Hindsight Instruction Pairing (Section 4.1), a method for pairing large amounts of diverse robot sensor data with relevant human language. To leverage both image goal and language goal datasets, we introduce Multicontext Imitation Learning (Section 4.2). In Section 4.3, we describe LangLfP which ties together

these components to learn a single policy that follows many human instructions over a long horizon.

4.1. Pairing play with human language

From a statistical machine learning perspective, an obvious candidate for grounding human language in robot sensor data is a large corpora of robot sensor data paired with relevant language. One way to collect this data is to choose an instruction, then collect optimal behavior. Instead we sample any robot behavior from play, then collect an optimal instruction. We call this Hindsight Instruction Pairing (Algorithm 3, part 1 of Figure 1). Just like how a hindsight goal image is an after-the-fact answer to the question “which goal state makes this trajectory optimal?”, a *hindsight instruction* is an after-the-fact answer to the question “which language instruction makes this trajectory optimal?”. We obtain these pairs by showing humans onboard robot sensor videos, then asking them “what instruction would you give the agent to get from first frame to last frame”?

Concretely, our pairing process assumes access to D_{play} , obtained using Algorithm 2 and a pool of non-expert human overseers. From D_{play} , we create a new dataset $D_{(\text{play}, \text{lang})} = \{(\tau, l)_i\}_{i=0}^{D_{(\text{play}, \text{lang})}}$, consisting of short-horizon play sequences τ paired with $l \in L$ a human-provided hindsight instruction with no restrictions on vocabulary or grammar.

This process is scalable because pairing happens after-the-fact, making it straightforward to parallelize via crowdsourcing. The language collected is also naturally rich, as it sits on top of play and is similarly not constrained by an upfront task definition. This results in instructions for functional behavior (e.g. “open the drawer”, “press the green button”), as well as general non task-specific behavior (e.g. “move your hand slightly to the left.” or “do nothing.”) See more real examples in Table 5 and video examples of our training data [here](#). Crucially, we do not need pair every experience from play with language to learn to follow instructions. This is made possible with Multicontext Imitation Learning, described next.

4.2. Multicontext Imitation Learning

So far, we have described a way to create two contextual imitation datasets: D_{play} holding hindsight goal image examples and $D_{(\text{play}, \text{lang})}$, holding hindsight instruction examples. Ideally, we could train a single policy that is agnostic to either task description. This would allow us to share statistical strength over multiple datasets during training, then free us to use just language specification at test time.

With this motivation, we introduce *multicontext imitation learning* (MCIL), a simple and universally applicable generalization of contextual imitation to multiple heterogeneous

Algorithm 1 Multicontext imitation learning

```
1: Input:  $\mathcal{D} = \{D^0, \dots, D^K\}$ ,  $D^k = \{(\tau_i^k, c_i^k)\}_{i=0}^{D^k}$ , One
   dataset per context type (e.g. goal image, language in-
   struction, task id), each holding pairs of (demonstration,
   context).
2: Input:  $\mathcal{F} = \{f_\theta^0, \dots, f_\theta^K\}$ , One encoder per context
   type, mapping context to shared latent goal space, e.g.
    $z = f_\theta^k(c^k)$ .
3: Input:  $\pi_\theta(a_t|s_t, z)$ , Single latent goal conditioned pol-
   icy.
4: Input: Randomly initialize parameters  $\theta =$ 
    $\{\theta_\pi, \theta_{f^0}, \dots, \theta_{f^K}\}$ 
5: while True do
6:    $\mathcal{L}_{\text{MCIL}} \leftarrow 0$ 
7:   # Loop over datasets.
8:   for  $k = 0 \dots K$  do
9:     # Sample a (demonstration, context) batch from
     this dataset.
10:     $(\tau^k, c^k) \sim D^k$ 
11:    # Encode context in shared latent goal space.
12:     $z = f_\theta^k(c^k)$ 
13:    # Accumulate imitation loss.
14:     $\mathcal{L}_{\text{MCIL}} += \sum_{t=0}^{|\tau^k|} \log \pi_\theta(a_t|s_t, z)$ 
15:   end for
16:   # Average gradients over context types.
17:    $\mathcal{L}_{\text{MCIL}} *= \frac{1}{|\mathcal{D}|}$ 
18:   # Train policy and all encoders end-to-end.
19:   Update  $\theta$  by taking a gradient step w.r.t.  $\mathcal{L}_{\text{MCIL}}$ 
20: end while
```

contexts. The main idea is to represent a large set of policies by a single, unified function approximator that generalises over states, tasks, and *task descriptions*. Concretely, MCIL assumes access to multiple imitation learning datasets $\mathcal{D} = \{D^0, \dots, D^K\}$, each with a different way of describing tasks. Each $D^k = \{(\tau_i^k, c_i^k)\}_{i=0}^{D^k}$ holds pairs of state-action trajectories τ paired with some context $c \in C$. For example, D^0 might contain demonstrations paired with one-hot task ids (a conventional multitask imitation learning dataset), D^1 might contain image goal demonstrations, and D^2 might contain language goal demonstrations.

Rather than train one policy per dataset, MCIL instead trains a single *latent goal* conditioned policy $\pi_\theta(a_t|s_t, z)$ over *all* datasets simultaneously, learning to map each task description type to the same latent goal space $z \in \mathbb{R}^d$. See Figure 2. This latent space can be seen as a common abstract goal representation shared across many imitation learning problems. To make this possible, MCIL assumes a set of parameterized encoders $\mathcal{F} = \{f_\theta^0, \dots, f_\theta^K\}$, one per dataset, each responsible for mapping task descriptions of a particular type to the common latent goal space, i.e. $z = f_\theta^k(c^k)$. For in-

stance these could be a task id embedding lookup, an image encoder, and a language encoder respectively.

MCIL has a simple training procedure: At each training step, for each dataset D^k in \mathcal{D} , sample a minibatch of trajectory-context pairs $(\tau^k, c^k) \sim D^k$, encode the contexts in latent goal space $z = f_\theta^k(c^k)$, then compute a simple maximum likelihood contextual imitation objective:

$$\mathcal{L}_{\text{context}}(D, h) = \mathbb{E}_{(\tau, c) \sim D} \left[\sum_{t=0}^{|\tau|} \log \pi_\theta(a_t|s_t, f_\theta(c)) \right] \quad (3)$$

The full MCIL objective averages this per-dataset objective over all datasets at each training step,

$$\mathcal{L}_{\text{MCIL}} = \frac{1}{|\mathcal{D}|} \sum_k \mathcal{L}_{\text{context}}(D_k, h_k) \quad (4)$$

and the policy and all goal encoders are trained end to end to maximize $\mathcal{L}_{\text{MCIL}}$. See Algorithm 1 for full minibatch training pseudocode.

Multicontext learning has properties that make it broadly useful beyond this paper. While we set $\mathcal{D} = \{D_{\text{play}}, D_{(\text{play}, \text{lang})}\}$ in this paper, this approach allows more generally for training over any set of imitation datasets with different descriptions—e.g. task id, language, human video demonstration, speech, etc. Being context-agnostic enables a highly efficient training scheme: learn the majority of control from the cheapest data source, while learning the most general form of task conditioning from a small number of labeled examples. In this way, multicontext learning can be interpreted as transfer learning through a shared goal space. We exploit this strategy in this work. Crucially, this can reduce the cost of human oversight to the point where it can be practically applied. Multicontext learning allows us to train an agent to follow human instructions with less than 1% of collected robot experience requiring paired language, with the majority of control learned instead from relabeled goal image data.

4.3. LangLFP: learning to follow image and human language goals.

We now have all the components to introduce *LangLFP* (language conditioned learning from play). LangLFP is a special case of multicontext imitation learning (Section 4.2) applied to our problem setting. At a high level, LangLFP trains a single multicontext policy $\pi_\theta(a_t|s_t, z)$ over datasets $\mathcal{D} = \{D_{\text{play}}, D_{(\text{play}, \text{lang})}\}$, consisting of hindsight goal image tasks and hindsight instruction tasks. We define $\mathcal{F} = \{g_{\text{enc}}, s_{\text{enc}}\}$, neural network encoders mapping from image goals and instructions respectively to the same latent *visuo-lingual* goal space. LangLFP learns perception, natural language understanding, and control end-to-end with no auxiliary losses. We discuss the separate modules below.

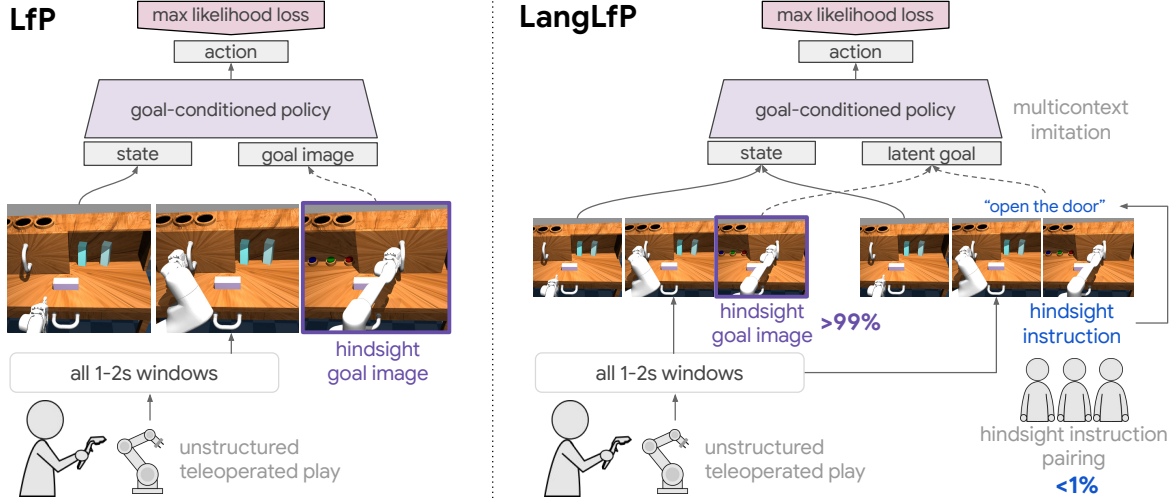


Figure 3: Comparing original goal image conditioned LfP (left) to goal image or natural language conditioned LangLfP (right). Both are trained on top of teleoperated play, relabeled into millions of goal image conditioned imitation examples. LangLfP is additionally trained on play windows paired with hindsight instructions. This multicontext training allows for the majority of control to be learned from self-supervision (>99% relabeled play), with <1% of play windows requiring language pairing.

Perception module. In our experiments, τ in each example consists of $\{(O_t, a_t)\}_t^{|\tau|}$, a sequence of onboard observations O_t and actions. Each observation contains a high-dimensional image and internal proprioceptive sensor reading. A learned perception module P_θ maps each observation tuple to a low-dimensional embedding, e.g. $s_t = P_\theta(O_t)$, fed to the rest of the network. See Appendix B.1 for details on our perception architecture. This perception module is shared with g_{enc} , which defines an additional network on top to map encoded goal observation s_g to a point in z space. See Appendix B.2 for details.

Language module. Our language goal encoder s_{enc} tokenizes raw text l into subwords (Sennrich et al., 2015), retrieves subword embeddings from a lookup table, then summarizes embeddings into a point in z space. Subword embeddings are randomly initialized at the beginning of training and learned end-to-end by the final imitation loss. See Appendix B.3 for s_{enc} implementation details.

Control module. While we could in principle use any architecture to implement the multicontext policy $\pi_\theta(a_t|s_t, z)$, we use Latent Motor Plans (LMP) (Lynch et al., 2019). LMP is a goal-directed imitation architecture that uses latent variables to model the large amount of multimodality inherent to freeform imitation datasets. Concretely, it is a sequence-to-sequence conditional variational autoencoder (seq2seq CVAE) autoencoding contextual demonstrations through a latent “plan” space. The decoder is a goal conditioned policy. As a CVAE, LMP lower bounds maximum likelihood contextual imitation (Equation 3.1), and is easily adapted to our multicontext setting. See Appendix B.4 for details on this module.

LangLfP training. Figure 3 compares LangLfP training to original LfP training. At each training step we sample a batch of image goal tasks from D_{play} and a batch of language goal tasks from $D_{(\text{play}, \text{lang})}$. Observations are encoded into state space using the perception module P_θ . Image and language goals are encoded into latent goal space z using encoders g_{enc} and s_{enc} . We then use $\pi_\theta(a_t|s_t, z)$ to compute the multicontext imitation objective, averaged over both task descriptions. We take a combined gradient step with respect to all modules—perception, language, and control—optimizing the whole architecture end-to-end as a single neural network. See details in Appendix B.5.

Following human instructions at test time. At the beginning of a test episode the agent receives as input its onboard observation O_t and a human-specified natural language goal l . The agent encodes l in latent goal space z using the trained sentence encoder s_{enc} . The agent then solves for the goal in closed loop, repeatedly feeding the current observation and goal to the learned policy $\pi_\theta(a|s_t, z)$, sampling actions, and executing them in the environment. The human operator can type a new language goal l at any time. See picture in part 3 of Figure 1.

4.4. Transferring knowledge from generic text corpora

Large “in the wild” natural language corpora reflect substantial human knowledge about the world (Zellers et al., 2018). Many recent works have successfully transferred this knowledge to downstream tasks in NLP via pretrained embeddings (Devlin et al., 2018; Radford et al., 2019; Raffel et al., 2019; Goldberg, 2019). Can we achieve similar knowledge transfer to *robotic manipulation*?

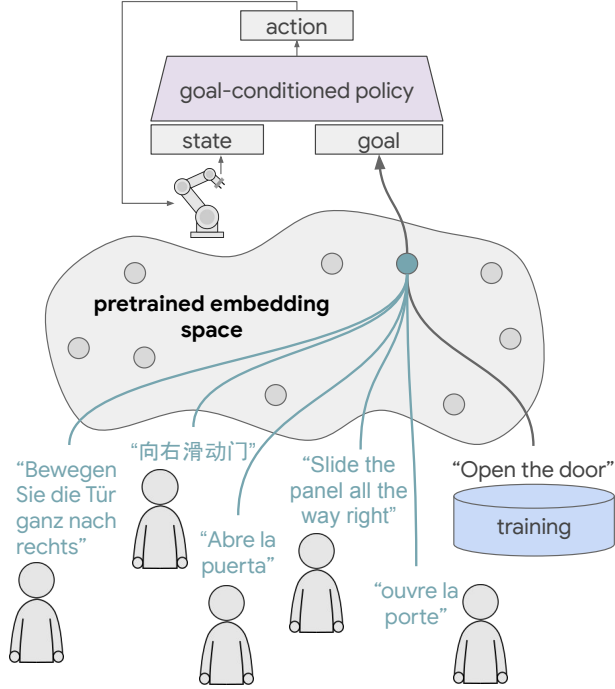


Figure 4: **Following novel instructions at test time in zero shot using transfer learning.** Simply by training on top of pretrained language embeddings, we can give a language conditioned policy the ability to follow out of distribution instructions in zero shot at test time. The pretrained embedding space is responsible for relating novel instructions (green) to ones the agent has been trained to follow (black).

We hypothesize two benefits to this type of transfer. First, if there is a semantic match between the source corpora and the target environment, more structured inputs may act as a strong prior, shaping grounding or control (Luketina et al., 2019). Second, language embeddings have been shown to encode similarity between large numbers of words and sentences. This may allow an agent to follow many novel instructions in zero shot, provided they are sufficiently “close” to ones it has been trained to follow (Figure 4). Note, given the complexity of natural language, it is likely that robots in open-world environments will need to be able to follow synonym commands outside of a particular training set.

To test these hypotheses, we introduce a simple transfer learning technique, generally applicable to any natural language conditioned agent. We assume access to a neural language model, pretrained on large unlabeled text corpora, capable of mapping full sentences l to points in a semantic vector space $v \in \mathbb{R}^d$. Transfer is enabled simply by encoding language inputs l to the policy at training and test time in v before feeding to the rest of the network. We augment LangLFP in this way, which we refer to as *TransferLangLFP*. See Appendix B.3 for details.

5. Experimental Setup

Our experiments aim to answer the following questions:

1. “Ask me anything” scenario: Can LangLFP train a single agent to solve many human language conditioned robotic manipulation tasks in a row? How does LangLFP compare to prior goal image conditioned LFP, which has less practical task specification? How does our model, trained on unlabeled play, compare to an identical architecture trained on conventional labeled multitask demonstrations?
2. Transfer from unlabeled text corpora: Can knowledge be transferred from text to downstream robotic manipulation? Does our transfer learning technique allow a policy to follow novel instructions in zero shot?

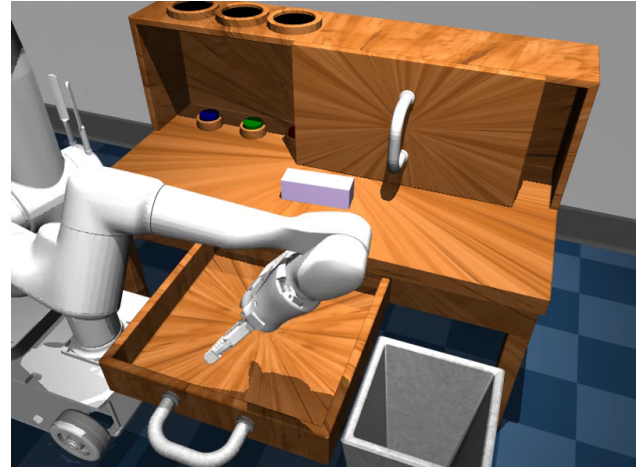


Figure 5: **Playroom environment:** A situated robot in a 3D MuJoCo environment.

5.1. 3D simulated environment

We conduct our experiments in the simulated 3D Playroom environment introduced in (Lynch et al., 2019), shown in Figure 5. The environment contains a desk with a sliding door and drawer that can be opened and closed. On the desk is a movable rectangular block and 3 buttons that can be pushed to control different colored lights. Next to the desk is a trash bin. Physics are simulated using the MuJoCo physics engine (Todorov et al., 2012). Videos here of play data collected in this environment give a good idea of the available complexity. In front of the desk is a realistic simulated 8-DOF robot (arm and parallel gripper). The agent perceives its surroundings from egocentric high-dimensional RGB video sensors. It additionally has access to continuous internal proprioceptive sensors, relaying the cartesian position and rotation of its end effector and gripper angles. We modify the environment to include a text

channel which the agent observes at each timestep, allowing humans to type unconstrained language commands. The agent must perform high-frequency, closed-loop continuous control to solve for user-described manipulation tasks, sending continuous position, rotation, and gripper commands to its arm at 30hz. See Appendix C for details.

5.2. Methods

In our experiments, we compare the following methods (more details in Appendix E):

- **LangBC** (“language, but no play”): a baseline natural language conditioned multitask imitation policy (Rahmatizadeh et al., 2018), trained on $D_{(\text{demo}, \text{lang})}$, 100 expert demonstrations for each of the 18 evaluation tasks paired with hindsight instructions.
- **LfP** (“play, but no language”): a baseline LfP model trained on D_{play} , conditioned on goal images at test time.
- **LangLfP (ours)** (“play and language”): Multicontext imitation trained on D_{play} and play paired with language $D_{(\text{play}, \text{lang})}$. Tasks are specified at test time using only natural language.
- **Restricted LangLfP**: To make a controlled comparison to LangBC, we train a baseline of LangLfP on “restricted D_{play} ”, a play dataset restricted to be the same size as $D_{(\text{demo}, \text{lang})}$. This restriction is artificial, as more unsegmented play can be collected with the same budget of time. This helps answer “for the same exact amount of data, which kind of data leads to better generalization: conventional multitask demonstrations, or relabeled play?”.
- **TransferLangLfP (ours)**: transfer learning augmented LangLfP, identical except instruction inputs are replaced with pretrained language embeddings.

We define two sets of experiments for each baseline: pixel experiments, where models receive high-dimensional image observations and must learn perception end-to-end, and state experiments, where models instead receive the ground truth simulator state consisting of positions and orientations for all objects in the scene. The latter provides an upper bound on how all well the various methods can learn language conditioned control, independent of a difficult perception problem (which may be improved upon independently with self-supervised representation learning methods (e.g. Sermanet et al. (2018); Oord et al. (2018); Ozair et al. (2019); Pirk et al. (2019))).

Note that all baselines can be seen as maximizing the same multicontext imitation objective, differing only on the particular composition of data sources. Therefore, to perform a

controlled comparison, we use the same imitation architecture (details in Sec. B) across all baselines. See Appendix D for a detailed description of all data sources.

6. “Ask Me Anything” Experiments

While one-off multitask evaluations (Yu et al., 2019; Lynch et al., 2019) are challenging and interesting, a realistic and significantly more difficult scenario is one in which a human gives a robot multiple instructions in a row over a *long horizon*, for example: “get the block from the shelf...now open the drawer...now sweep the block into the drawer...now close the drawer”. Furthermore, agents should be able to accomplish any subtask in any order. This demands a training process that adequately covers transitions between arbitrary pairs of tasks. This setting of long-horizon human language conditioned robotic manipulation has not yet been explored in the literature to our knowledge. While difficult, we believe it aligns well with test-time expectations for a learning robot in everyday environments.

6.1. Long-Horizon Evaluation

We define a long horizon evaluation by significantly expanding upon the previous 18-task evaluation in (Lynch et al., 2019), Multi-18. We construct many multi-stage evaluations by treating the original 18 tasks as subtasks, then consider all valid N-stage transitions between them. This results in 2-stage, 3-stage, and 4-stage long horizon manipulation benchmarks, referred to here as Chain-2, Chain-3, and Chain-4. Note that the number of unique tasks increases rapidly with N: there are 63 Chain-2 tasks, 254 Chain-3 tasks, and 925 Chain-4 tasks. Also note this multi-stage scenario subsumes the original Multi-18, which can be seen as just testing the first stage. This allows for direct comparison to prior work. See Appendix F for details on benchmark construction and evaluation walkthrough. We evaluate all methods on these long-horizon benchmarks and present the results in Table 1 and Figure 6, discussing our findings below. Success is reported with confidence intervals over 3 seeded training runs.

6.2. Long Horizon Results

Goal image conditioned comparison. In Table 1, we find that LangLfP matches the performance of LfP on all benchmarks within margin of error, but does so with entirely from natural language task specification. Notably, this is achieved with only $\sim 0.1\%$ of play requiring language pairing, with the majority of control still learned from self-supervised imitation. This is important because it shows our simple framework allows open-ended robotic manipulation to be combined with open-ended text conditioning with minimal additional human supervision. This was the main question of this work. We attribute these results to our multicontext

Method	Input	Training source	Task conditioning	Multi-18 Success (18 tasks)	Chain-4 Success (925 long-horizon tasks)
LangBC	pixels	predefined demos	text	20.0% \pm 3.0	7.1% \pm 1.5
Restricted LangLfP	pixels	play	text	47.1% \pm 2.0	25.0% \pm 2.0
LfP	pixels	play	goal image	66.4% \pm 2.2	53.0% \pm 5.0
LangLfP (ours)	pixels	play	text	68.6% \pm 1.7	52.1% \pm 2.0
TransferLangLfP (ours)	pixels	play	text	74.1% \pm 1.5	68.6% \pm 1.6
LangBC	states	predefined demos	text	38.5% \pm 6.3	13.9% \pm 1.4
Restricted LangLfP	states	play	text	88.0% \pm 1.4	64.2% \pm 1.5
LangLfP (ours)	states	play	text	88.5% \pm 2.9	63.2% \pm 0.9
TransferLangLfP (ours)	states	play	text	90.5% \pm 0.8	71.8% \pm 1.6

Table 1: **“Ask Me Anything” experiments:** long horizon, natural language conditioned visual manipulation with a human in the loop. We report the percentage of subtasks completed for one-off instructions (Multi-18) and four instructions in a row (Chain-4). We see that LangLfP matches the performance of LfP, but has a more scalable form of task conditioning. Additionally we see TransferLangLfP significantly benefits from knowledge transfer from generic text corpora, outperforming LangLfP and original LfP. Finally, models trained on unstructured play significantly outperform LangBC, trained on predefined task demonstrations, especially in the long horizon.

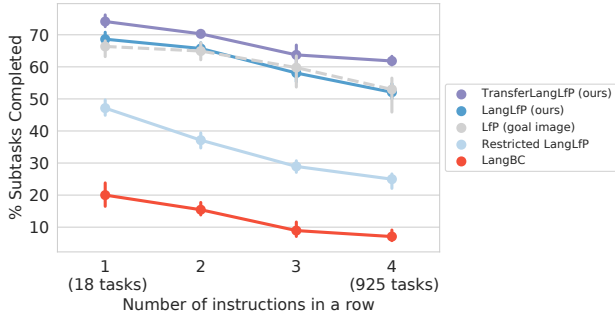


Figure 6: **Multitask human language conditioned visual manipulation over a long horizon.** Here we plot the performance of all methods as a human gives a sequence of natural language instructions to follow. Note there are 18 single instruction tasks, rising to 925 unique four instruction tasks. The x-axis considers the number of instructions given in a row and the y-axis considers the percentage of instructions successfully completed. We also plot goal image conditioned LfP performance for comparison.

learning setup, which allows statistical strength to be shared over multiple datasets, some plentiful and some scarce.

Conventional multitask imitation comparison. We see in Table 1 and Fig. 6 that LangLfP outperforms LangBC on every benchmark. Notably, this result holds even when the play dataset is artificially restricted to the same size as the conventional demonstration dataset (Restricted LangLfP vs LangBC). This is important because it shows that models trained on top of relabeled play generalize much better than those trained on narrow predefined task demonstrations, especially in the most difficult long horizon setting. Qualitatively (videos), the difference between the training sources is striking. We find that play-trained policies can of transition well between tasks and recover from initial failures, while narrow demo-trained policies quickly encounter

compounding imitation error and never recover. We believe this highlights the importance of training data that covers state space, including large numbers of tasks as well as non task-specific behavior like transitions.

Following 15 instructions in a row. We present qualitative results (video) showing that our agent can follow 15 natural language instructions in a row provided by a human. We believe this offers strong encouragement that simple high capacity imitation learning can be competitive with more complicated long horizon reinforcement learning methods.

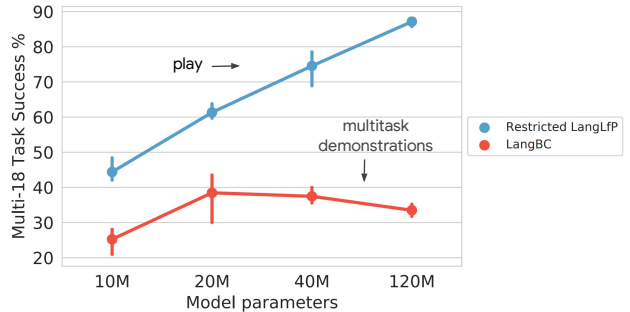


Figure 7: **Play scales with model capacity.** Large model capacity is well utilized to absorb diversity in unstructured play, but is wasted on an equivalent amount of conventional predefined task demonstrations.

Play scales with model capacity. In Figure 7, we consider task performance as a function of model size for models trained on play or conventional predefined demonstrations. For fair comparison, we compare LangBC to Restricted LangLfP, trained on the same amount of data. We study both models from state inputs to understand upper bound performance. As we see, performance steadily improves as model size is increased for models trained on play, but peaks and then declines for models trained on conventional demonstrations. Our interpretation is that larger capacity is

effectively utilized to absorb the diversity in play, whereas additional capacity is wasted on equivalently sized datasets constrained to predefined behaviors. This suggests that the simple recipe of collecting large play datasets and scaling up model capacity to achieve higher performance is a valid one.

Language unlocks human assistance. Natural language conditioned control allows for new modes of interactive test time behavior, allowing humans to give guidance to agents at test time that would be impractical to give via goal image or task id conditioned control. See [this video](#) and Sec. G.2 for a concrete example. During the long horizon evaluation, the arm of the agent becomes stuck on top of the desk shelf. The operator is able to quickly specify a new subtask “pull your arm back”, which the agent completes, leaving it in a much better initialization to complete the original task. This rapid interactive guidance would have required having a corresponding goal image on hand for “pull your arm back” in the image conditioned scenario or would have required learning an entire separate task using demonstrations in the task id conditioned scenario. Section G additionally shows how humans can quickly compose new tasks not in the 18-task benchmark with language, like “put the block in the trash bin”.

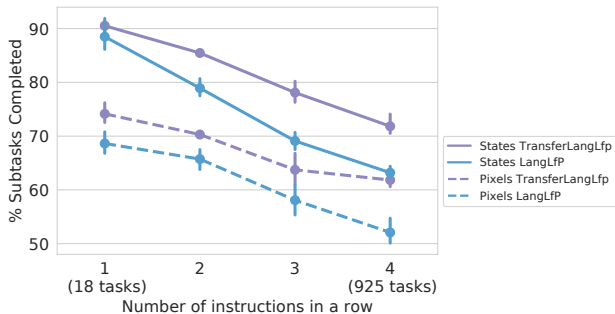


Figure 8: **Knowledge transfer from generic text corpora to robotic manipulation.** TransferLangLfp, which trains on top of pretrained language embeddings, systematically outperforms LangLfp, which learns language understanding from scratch, on all manipulation benchmarks.

Method	OOD-syn (~15k tasks)	OOD-16-lang (~240k tasks)
Random Policy	0.0% \pm 0.0	0.0% \pm 0.0
LangLfp	37.6% \pm 2.3	27.94% \pm 3.5
TransferLangLfp	60.2% \pm 3.2	56.0% \pm 1.4

Table 2: **Following out of distribution instructions:** Training on top of pretrained neural embeddings (TransferLangLfp) allows our agent to follow thousands of out-of-distribution synonym instructions in 16 languages in zero shot.

7. Knowledge Transfer Experiments

Here we evaluate our transfer learning augmentation to LangLfp. In these experiments, we are interested in two questions: 1) Is knowledge transfer possible from generic text corpora to language-guided robotic manipulation? 2) Does training on top of pretrained embeddings allow our policy to follow instructions it has never been trained on?

7.1. Knowledge Transfer Results

Positive transfer to robotic manipulation. In Table 1 and Figure 8, we see that while LangLfp and prior Lfp perform comparably, TransferLangLfp systematically outperforms both. This is important because it shows the first evidence, to our knowledge, that world knowledge reflected in large unstructured bodies of text can be transferred downstream to improve language-guided robotic manipulation. As mentioned in (Luketina et al., 2019), we hypothesize this transfer is possible because we conduct experiments in a 3D environment with realistic object interactions, matching the semantics of those described in real world textual corpora.

Following out of distribution “synonym instructions”. To study whether our proposed transfer augmentation allows an agent to follow out-of-distribution instructions, we replace one or more words in each Multi-18 instruction with a synonym outside training, e.g. “drag the block from the shelf” \rightarrow “retrieve the brick from the cupboard”. Enumerating all substitutions results in a set of 14,609 out-of-distribution instructions covering all 18 tasks. We evaluate a random policy, LangLfp, and TransferLangLfp on this benchmark, OOD-syn, reporting the results in Table 2. Success is reported with confidence intervals over 3 seeded training runs. We see while LangLfp is able to solve some novel tasks by inferring meaning from context (e.g. ‘pick up the block’ and ‘pick up the brick’ might reasonably map to the same task), its performance degrades significantly. TransferLangLfp on the other hand, generalizes substantially better. This shows that the simple transfer learning technique we propose greatly magnifies the test time scope of an instruction following agent, allowing it to follow thousands more user instructions than it was trained with. Given the inherent complexity of language, this is an important real world consideration.

Following out of distribution instructions in 16 different languages. Here we study a rather extreme case of out-of-distribution generalization: following instructions in languages not seen during training (e.g. French, Mandarin, German, etc.). To study this, we combine the original set of test instructions from Multi-18 with the expanded synonym instruction set OOD-syn, then translate both into 16 languages using the Google translate API. This results in ~240k out-of-distribution instructions covering all 18 tasks. We evaluate the previous methods on this cross-lingual ma-

nipulation benchmark, OOD-16-lang, reporting success in Table 2. We see that when LangLFP receives instructions with no training overlap, it resorts to producing maximum likelihood play actions. This results in some spurious task success, but performance degrades materially. Remarkably, TransferLangLFP solves a substantial portion of these in zero shot, degrading only slightly from the english-only benchmark. See [videos](#) of TransferLangLFP following instructions in 16 novel languages. These results show that simply training high capacity imitation policies on top of pretrained embedding spaces affords agents powerful zero shot generalization capabilities. While practically, one could imagine simply translating these instructions first into English before feeding them to our system, this demonstrates that a large portion of the necessary analogical reasoning can happen internal to the agent in a manner that is end-to-end differentiable. While in this paper we do not finetune the embeddings in this manner, an exciting direction for future work would be to see if grounding language embeddings in embodied imitation improves representation learning over text-only inputs.

8. Limitations and Future Work

Although the coverage of play mitigates failure modes in conventional imitation setups, we observe several limitations in our policies at test time. In this [video](#), we see the policy make multiple attempts to solve the task, but times out before it is able to do so. We see in this [video](#) that the agent encounters a particular kind of compounding error, where the arm flips into an awkward configuration, likely avoided by humans during teleoperated play. This is potentially mitigated by a more stable choice of rotation representation, or more varied play collection. We note that the human is free to help the agent out of these awkward configurations using language assistance, as demonstrated in Sec. G.2. More examples of failures can be seen [here](#).

While LangLFP relaxes important constraints around task specification, it is fundamentally a goal-directed imitation method and lacks a mechanism for autonomous policy improvement. An exciting area for future work may be one that combines the coverage of teleoperated play, the scalability and flexibility of multicontext imitation pretraining, and the autonomous improvement of reinforcement learning, similar to prior successful combinations of LfP and RL (Gupta et al., 2019).

As in original LfP, the scope of this work is task-agnostic control in a single environment. We note this is consistent with the standard imitation assumptions that training and test tasks are drawn i.i.d. from the same distribution. An interesting question for future work is whether training on a large play corpora covering many rooms and objects allows for generalization to unseen rooms or objects.

Simple maximum likelihood makes it easy to learn large capacity perception and control architectures end-to-end. It additionally enjoys significant sample efficiency and stability benefits over multitask RL at the moment (Schaul et al., 2019). We believe these properties provide good motivation for continuing to scale larger end-to-end imitation architectures over larger play datasets as a practical strategy for task-agnostic control.

9. Conclusion

Robots that can learn to relate human language to their perception and actions would be especially useful in open-world environments. This work asks: provided real humans play a direct role in this learning process, what is the most efficient way to go about it? With this motivation, we introduced LangLFP, an extension of LfP trained both on relabeled goal image play and play paired with human language instructions. To reduce the cost of language pairing, we introduced Multicontext Imitation Learning, which allows a single policy to be trained over both goal image and language tasks, then use just language conditioning at test time. Crucially, this made it so that less than 1% collected robot experience required language pairing to enable the new mode of conditioning. In experiments, we found that a single policy trained with LangLFP can solve many 3D robotic manipulation tasks over a long horizon, from onboard sensors, and specified only via human language. This represents a considerably more complex scenario than prior work in instruction following. Finally, we introduced a simple technique allowing for knowledge transfer from large unlabeled text corpora to robotic manipulation. We found that this significantly improved downstream visual control—the first instance to our knowledge of this kind of transfer. It also equipped our agent with the ability to follow thousands of instructions outside its training set in zero shot, in 16 different languages.

Acknowledgments

We thank Karol Hausman, Eric Jang, Mohi Khansari, Kanishka Rao, Jonathan Thompson, Luke Metz, Anelia Angelova, Sergey Levine, and Vincent Vanhoucke for providing helpful feedback on this manuscript. We additionally thank the overseers for providing paired language instructions.

References

- Jacob Andreas, Dan Klein, and Sergey Levine. Modular multitask reinforcement learning with policy sketches, 2016.
- Marcin Andrychowicz, Filip Wolski, Alex Ray, Jonas Schneider, Rachel Fong, Peter Welinder, Bob McGrew, Josh Tobin, OpenAI Pieter Abbeel, and Wojciech Zaremba. Hindsight experience replay. In *Advances in neural information processing systems*, pages 5048–5058, 2017.

- OpenAI: Marcin Andrychowicz, Bowen Baker, Maciek Chociej, Rafal Jozefowicz, Bob McGrew, Jakub Pachocki, Arthur Petron, Matthias Plappert, Glenn Powell, Alex Ray, et al. Learning dexterous in-hand manipulation. *The International Journal of Robotics Research*, 39(1):3–20, 2020.
- Brenna D Argall, Sonia Chernova, Manuela Veloso, and Brett Browning. A survey of robot learning from demonstration. *Robotics and autonomous systems*, 57(5):469–483, 2009.
- Christopher G Atkeson and Stefan Schaal. Robot learning from demonstration. In *ICML*, volume 97, pages 12–20. Citeseer, 1997.
- Dare Baldwin and Meredith Meyer. How inherently social is language? 2007.
- Yonatan Bisk, Ari Holtzman, Jesse Thomason, Jacob Andreas, Yoshua Bengio, Joyce Chai, Mirella Lapata, Angeliki Lazaridou, Jonathan May, Aleksandr Nisnevich, Nicolas Pinto, and Joseph Turian. Experience grounds language, 2020.
- Rich Caruana. Multitask learning. *Machine learning*, 28(1):41–75, 1997.
- Devendra Singh Chaplot, Kanthashree Mysore Sathyendra, Rama Kumar Pasumarthi, Dheeraj Rajagopal, and Ruslan Salakhutdinov. Gated-attention architectures for task-oriented language grounding. In *Thirty-Second AAAI Conference on Artificial Intelligence*, 2018.
- Herbert H Clark and Susan E Brennan. Grounding in communication. 1991.
- Abhishek Das, Samyak Datta, Georgia Gkioxari, Stefan Lee, Devi Parikh, and Dhruv Batra. Embodied question answering. In *Proceedings of the IEEE Conference on Computer Vision and Pattern Recognition Workshops*, pages 2054–2063, 2018.
- Jacob Devlin, Ming-Wei Chang, Kenton Lee, and Kristina Toutanova. Bert: Pre-training of deep bidirectional transformers for language understanding. *arXiv preprint arXiv:1810.04805*, 2018.
- Yiming Ding, Carlos Florensa, Pieter Abbeel, and Mariano Phielipp. Goal-conditioned imitation learning. In *Advances in Neural Information Processing Systems*, pages 15298–15309, 2019.
- Yan Duan, Marcin Andrychowicz, Bradly Stadie, OpenAI Jonathan Ho, Jonas Schneider, Ilya Sutskever, Pieter Abbeel, and Wojciech Zaremba. One-shot imitation learning. In *Advances in neural information processing systems*, pages 1087–1098, 2017.
- Frederik Ebert, Chelsea Finn, Sudeep Dasari, Annie Xie, Alex Lee, and Sergey Levine. Visual foresight: Model-based deep reinforcement learning for vision-based robotic control. *arXiv preprint arXiv:1812.00568*, 2018.
- Benjamin Eysenbach, Xinyang Geng, Sergey Levine, and Ruslan Salakhutdinov. Rewriting history with inverse rl: Hind-sight inference for policy improvement. *arXiv preprint arXiv:2002.11089*, 2020.
- Carlos Florensa, Jonas Degraeve, Nicolas Heess, Jost Tobias Springenberg, and Martin Riedmiller. Self-supervised learning of image embedding for continuous control. *arXiv preprint arXiv:1901.00943*, 2019.
- Dibya Ghosh, Abhishek Gupta, Justin Fu, Ashwin Reddy, Coline Devine, Benjamin Eysenbach, and Sergey Levine. Learning to reach goals without reinforcement learning. *arXiv preprint arXiv:1912.06088*, 2019.
- Yoav Goldberg. Assessing bert’s syntactic abilities, 2019.
- Prasoon Goyal, Scott Niekum, and Raymond J. Mooney. Using natural language for reward shaping in reinforcement learning, 2019.
- Shixiang Gu, Ethan Holly, Timothy Lillicrap, and Sergey Levine. Deep reinforcement learning for robotic manipulation with asynchronous off-policy updates. In *2017 IEEE international conference on robotics and automation (ICRA)*, pages 3389–3396. IEEE, 2017.
- Abhishek Gupta, Vikash Kumar, Corey Lynch, Sergey Levine, and Karol Hausman. Relay policy learning: Solving long horizon tasks via imitation and reinforcement learning. *Conference on Robot Learning (CoRL)*, 2019.
- David Ha and Jürgen Schmidhuber. World models. *arXiv preprint arXiv:1803.10122*, 2018.
- Tuomas Haarnoja, Aurick Zhou, Kristian Hartikainen, George Tucker, Sehoon Ha, Jie Tan, Vikash Kumar, Henry Zhu, Abhishek Gupta, Pieter Abbeel, et al. Soft actor-critic algorithms and applications. *arXiv preprint arXiv:1812.05905*, 2018.
- Danijar Hafner, Timothy Lillicrap, Ian Fischer, Ruben Villegas, David Ha, Honglak Lee, and James Davidson. Learning latent dynamics for planning from pixels. *arXiv preprint arXiv:1811.04551*, 2018.
- Ankur Handa, Karl Van Wyk, Wei Yang, Jacky Liang, Yu-Wei Chao, Qian Wan, Stan Birchfield, Nathan Ratliff, and Dieter Fox. Dex-pilot: Vision based teleoperation of dexterous robotic hand-arm system. *arXiv preprint arXiv:1910.03135*, 2019.
- Stevan Harnad. The symbol grounding problem. *Physica D: Nonlinear Phenomena*, 42(1-3):335–346, 1990.
- Karl Moritz Hermann, Felix Hill, Simon Green, Fumin Wang, Ryan Faulkner, Hubert Soyer, David Szepesvari, Wojciech Marjan Czarnecki, Max Jaderberg, Denis Teplyashin, et al. Grounded language learning in a simulated 3d world. *arXiv preprint arXiv:1706.06551*, 2017.
- Todd Hester, Matej Vecerik, Olivier Pietquin, Marc Lanctot, Tom Schaul, Bilal Piot, Dan Horgan, John Quan, Andrew Sendonaris, Ian Osband, et al. Deep q-learning from demonstrations. In *Thirty-Second AAAI Conference on Artificial Intelligence*, 2018.
- Felix Hill, Andrew Lampinen, Rosalia Schneider, Stephen Clark, Matthew Botvinick, James L McClelland, and Adam Santoro. Emergent systematic generalization in a situated agent. *arXiv preprint arXiv:1910.00571*, 2019.
- Jeremy Howard and Sebastian Ruder. Universal language model fine-tuning for text classification, 2018.
- Yiding Jiang, Shixiang Gu, Kevin Murphy, and Chelsea Finn. Language as an abstraction for hierarchical deep reinforcement learning, 2019.
- Leslie Pack Kaelbling. Learning to achieve goals. In *IJCAI*, pages 1094–1099. Citeseer, 1993.

- Dmitry Kalashnikov, Alex Irpan, Peter Pastor, Julian Ibarz, Alexander Herzog, Eric Jang, Deirdre Quillen, Ethan Holly, Mrinal Kalakrishnan, Vincent Vanhoucke, et al. Qt-opt: Scalable deep reinforcement learning for vision-based robotic manipulation. *arXiv preprint arXiv:1806.10293*, 2018.
- Jens Kober, J Andrew Bagnell, and Jan Peters. Reinforcement learning in robotics: A survey. *The International Journal of Robotics Research*, 32(11):1238–1274, 2013.
- Thomas Kollar, Stefanie Tellex, Deb Roy, and Nicholas Roy. Toward understanding natural language directions. In *2010 5th ACM/IEEE International Conference on Human-Robot Interaction (HRI)*, pages 259–266. IEEE, 2010.
- J Zico Kolter and Andrew Y Ng. Near-bayesian exploration in polynomial time. In *Proceedings of the 26th annual international conference on machine learning*, pages 513–520, 2009.
- Lisa Lee, Benjamin Eysenbach, Emilio Parisotto, Eric Xing, Sergey Levine, and Ruslan Salakhutdinov. Efficient exploration via state marginal matching. *arXiv preprint arXiv:1906.05274*, 2019.
- Sergey Levine, Chelsea Finn, Trevor Darrell, and Pieter Abbeel. End-to-end training of deep visuomotor policies. *The Journal of Machine Learning Research*, 17(1):1334–1373, 2016.
- Jelena Luketina, Nantas Nardelli, Gregory Farquhar, Jakob Foerster, Jacob Andreas, Edward Grefenstette, Shimon Whiteson, and Tim Rocktäschel. A survey of reinforcement learning informed by natural language. *arXiv preprint arXiv:1906.03926*, 2019.
- Corey Lynch, Mohi Khansari, Ted Xiao, Vikash Kumar, Jonathan Tompson, Sergey Levine, and Pierre Sermanet. Learning latent plans from play. *Conference on Robot Learning (CoRL)*, 2019. URL <https://arxiv.org/abs/1903.01973>.
- Matt MacMahon, Brian Stankiewicz, and Benjamin Kuipers. Walk the talk: Connecting language, knowledge, and action in route instructions. *Def*, 2(6):4, 2006.
- Dipendra Misra, John Langford, and Yoav Artzi. Mapping instructions and visual observations to actions with reinforcement learning. *arXiv preprint arXiv:1704.08795*, 2017.
- Raymond J Mooney. Learning to connect language and perception. In *AAAI*, pages 1598–1601, 2008.
- Ashvin Nair, Shikhar Bahl, Alexander Khazatsky, Vitchyr Pong, Glen Berseth, and Sergey Levine. Contextual imagined goals for self-supervised robotic learning. *arXiv preprint arXiv:1910.11670*, 2019.
- Ashvin V Nair, Vitchyr Pong, Murtaza Dalal, Shikhar Bahl, Steven Lin, and Sergey Levine. Visual reinforcement learning with imagined goals. In *Advances in Neural Information Processing Systems*, pages 9191–9200, 2018.
- Junhyuk Oh, Xiaoxiao Guo, Honglak Lee, Richard L Lewis, and Satinder Singh. Action-conditional video prediction using deep networks in atari games. In *Advances in neural information processing systems*, pages 2863–2871, 2015.
- Junhyuk Oh, Satinder Singh, Honglak Lee, and Pushmeet Kohli. Zero-shot task generalization with multi-task deep reinforcement learning. In *Proceedings of the 34th International Conference on Machine Learning-Volume 70*, pages 2661–2670. JMLR. org, 2017.
- Aaron van den Oord, Yazhe Li, and Oriol Vinyals. Representation learning with contrastive predictive coding. *arXiv preprint arXiv:1807.03748*, 2018.
- Pierre-Yves Oudeyer, Frederic Kaplan, et al. How can we define intrinsic motivation. In *Proc. of the 8th Conf. on Epigenetic Robotics*, volume 5, pages 29–31, 2008.
- Sherjil Ozair, Corey Lynch, Yoshua Bengio, Aaron Van den Oord, Sergey Levine, and Pierre Sermanet. Wasserstein dependency measure for representation learning. In *Advances in Neural Information Processing Systems*, pages 15578–15588, 2019.
- Emilio Parisotto, Jimmy Lei Ba, and Ruslan Salakhutdinov. Actor-mimic: Deep multitask and transfer reinforcement learning. *arXiv preprint arXiv:1511.06342*, 2015.
- Deepak Pathak, Pulkit Agrawal, Alexei A Efros, and Trevor Darrell. Curiosity-driven exploration by self-supervised prediction. In *Proceedings of the IEEE Conference on Computer Vision and Pattern Recognition Workshops*, pages 16–17, 2017.
- Sören Pirk, Mohi Khansari, Yunfei Bai, Corey Lynch, and Pierre Sermanet. Online object representations with contrastive learning. *arXiv preprint arXiv:1906.04312*, 2019.
- Vitchyr Pong, Shixiang Gu, Murtaza Dalal, and Sergey Levine. Temporal difference models: Model-free deep rl for model-based control. *arXiv preprint arXiv:1802.09081*, 2018.
- Vitchyr H Pong, Murtaza Dalal, Steven Lin, Ashvin Nair, Shikhar Bahl, and Sergey Levine. Skew-fit: State-covering self-supervised reinforcement learning. *arXiv preprint arXiv:1903.03698*, 2019.
- Ivaylo Popov, Nicolas Heess, Timothy Lillicrap, Roland Hafner, Gabriel Barth-Maron, Matej Vecerik, Thomas Lampe, Yuval Tassa, Tom Erez, and Martin Riedmiller. Data-efficient deep reinforcement learning for dexterous manipulation. *arXiv preprint arXiv:1704.03073*, 2017.
- Alec Radford, Jeffrey Wu, Rewon Child, David Luan, Dario Amodei, and Ilya Sutskever. Language models are unsupervised multitask learners. *OpenAI Blog*, 1(8):9, 2019.
- Colin Raffel, Noam Shazeer, Adam Roberts, Katherine Lee, Sharan Narang, Michael Matena, Yanqi Zhou, Wei Li, and Peter J Liu. Exploring the limits of transfer learning with a unified text-to-text transformer. *arXiv preprint arXiv:1910.10683*, 2019.
- Rouhollah Rahmatizadeh, Pooya Abolghasemi, Ladislau Böllöni, and Sergey Levine. Vision-based multi-task manipulation for inexpensive robots using end-to-end learning from demonstration. In *2018 IEEE International Conference on Robotics and Automation (ICRA)*, pages 3758–3765. IEEE, 2018.
- Aravind Rajeswaran, Vikash Kumar, Abhishek Gupta, Giulia Vezzani, John Schulman, Emanuel Todorov, and Sergey Levine. Learning complex dexterous manipulation with deep reinforcement learning and demonstrations. *arXiv preprint arXiv:1709.10087*, 2017.

- Jacqueline Sachs, Barbara Bard, and Marie L Johnson. Language learning with restricted input: Case studies of two hearing children of deaf parents. *Applied Psycholinguistics*, 2(1):33–54, 1981.
- Tim Salimans, Andrej Karpathy, Xi Chen, and Diederik P. Kingma. Pixelcnn++: Improving the pixelcnn with discretized logistic mixture likelihood and other modifications, 2017.
- Tom Schaul, Daniel Horgan, Karol Gregor, and David Silver. Universal value function approximators. In *International conference on machine learning*, pages 1312–1320, 2015.
- Tom Schaul, Diana Borsa, Joseph Modayil, and Razvan Pascanu. Ray interference: a source of plateaus in deep reinforcement learning. *arXiv preprint arXiv:1904.11455*, 2019.
- Jrgen Schmidhuber. Formal theory of creativity, fun, and intrinsic motivation (1990-2010). *IEEE Trans. Autonomous Mental Development*, 2(3):230–247, 2010. URL <http://dblp.uni-trier.de/db/journals/tamd/tamd2.html#Schmidhuber10>.
- Rico Sennrich, Barry Haddow, and Alexandra Birch. Neural machine translation of rare words with subword units. *arXiv preprint arXiv:1508.07909*, 2015.
- Pierre Sermanet, Kelvin Xu, and Sergey Levine. Unsupervised perceptual rewards for imitation learning. *Proceedings of Robotics: Science and Systems (RSS)*, 2017. URL <http://arxiv.org/abs/1612.06699>.
- Pierre Sermanet, Corey Lynch, Yevgen Chebotar, Jasmine Hsu, Eric Jang, Stefan Schaal, and Sergey Levine. Time-contrastive networks: Self-supervised learning from video. *Proceedings of International Conference in Robotics and Automation (ICRA)*, 2018. URL <http://arxiv.org/abs/1704.06888>.
- Mohit Shridhar, Jesse Thomason, Daniel Gordon, Yonatan Bisk, Winson Han, Roozbeh Mottaghi, Luke Zettlemoyer, and Dieter Fox. ALFRED: A Benchmark for Interpreting Grounded Instructions for Everyday Tasks. In *The IEEE Conference on Computer Vision and Pattern Recognition (CVPR)*, 2020. URL <https://arxiv.org/abs/1912.01734>.
- Avi Singh, Larry Yang, Kristian Hartikainen, Chelsea Finn, and Sergey Levine. End-to-end robotic reinforcement learning without reward engineering. *arXiv preprint arXiv:1904.07854*, 2019.
- Avi Singh, Eric Jang, Alexander Irpan, Daniel Kappler, Murtaza Dalal, Sergey Levine, Mohi Khansari, and Chelsea Finn. Scalable multi-task imitation learning with autonomous improvement. *arXiv preprint arXiv:2003.02636*, 2020.
- Burrhus Frederic Skinner. *Verbal behavior*. New York: Appleton-Century-Crofts, 1957.
- Linda Smith and Michael Gasser. The development of embodied cognition: Six lessons from babies. *Artificial life*, 11(1-2): 13–29, 2005.
- Chuanqi Tan, Fuchun Sun, Tao Kong, Wenchang Zhang, Chao Yang, and Chunfang Liu. A survey on deep transfer learning. In *International conference on artificial neural networks*, pages 270–279. Springer, 2018.
- Yee Teh, Victor Bapst, Wojciech M Czarnecki, John Quan, James Kirkpatrick, Raia Hadsell, Nicolas Heess, and Razvan Pascanu. Distral: Robust multitask reinforcement learning. In *Advances in Neural Information Processing Systems*, pages 4496–4506, 2017.
- Ian Tenney, Patrick Xia, Berlin Chen, Alex Wang, Adam Poliak, R Thomas McCoy, Najoung Kim, Benjamin Van Durme, Samuel R. Bowman, Dipanjan Das, and Ellie Pavlick. What do you learn from context? probing for sentence structure in contextualized word representations, 2019.
- Sebastian B Thrun. Efficient exploration in reinforcement learning. 1992.
- Emanuel Todorov, Tom Erez, and Yuval Tassa. Mujoco: A physics engine for model-based control. In *IROS*, pages 5026–5033. IEEE, 2012. ISBN 978-1-4673-1737-5. URL <http://dblp.uni-trier.de/db/conf/iros/iros2012.html#TodorovET12>.
- Laura Verga and Sonja A Kotz. How relevant is social interaction in second language learning? *Frontiers in human neuroscience*, 7:550, 2013.
- Xin Wang, Qiuyuan Huang, Asli Celikyilmaz, Jianfeng Gao, Dinghan Shen, Yuan-Fang Wang, William Yang Wang, and Lei Zhang. Reinforced cross-modal matching and self-supervised imitation learning for vision-language navigation. In *Proceedings of the IEEE Conference on Computer Vision and Pattern Recognition*, pages 6629–6638, 2019.
- David Warde-Farley, Tom Van de Wiele, Tejas Kulkarni, Catalin Ionescu, Steven Hansen, and Volodymyr Mnih. Unsupervised control through non-parametric discriminative rewards. *arXiv preprint arXiv:1811.11359*, 2018.
- Terry Winograd. Understanding natural language. *Cognitive psychology*, 3(1):1–191, 1972.
- Yinfei Yang, Daniel Cer, Amin Ahmad, Mandy Guo, Jax Law, Noah Constant, Gustavo Hernandez Abrego, Steve Yuan, Chris Tar, Yun-Hsuan Sung, et al. Multilingual universal sentence encoder for semantic retrieval. *arXiv preprint arXiv:1907.04307*, 2019.
- Haonan Yu, Haichao Zhang, and Wei Xu. A deep compositional framework for human-like language acquisition in virtual environment. *arXiv preprint arXiv:1703.09831*, 2017.
- Haonan Yu, Haichao Zhang, and Wei Xu. Interactive grounded language acquisition and generalization in a 2d world. *arXiv preprint arXiv:1802.01433*, 2018.
- Tianhe Yu, Deirdre Quillen, Zhanpeng He, Ryan Julian, Karol Hausman, Chelsea Finn, and Sergey Levine. Meta-world: A benchmark and evaluation for multi-task and meta reinforcement learning. *arXiv preprint arXiv:1910.10897*, 2019.
- Rowan Zellers, Yonatan Bisk, Roy Schwartz, and Yejin Choi. Swag: A large-scale adversarial dataset for grounded common-sense inference. *arXiv preprint arXiv:1808.05326*, 2018.
- Tianhao Zhang, Zoe McCarthy, Owen Jow, Dennis Lee, Xi Chen, Ken Goldberg, and Pieter Abbeel. Deep imitation learning for complex manipulation tasks from virtual reality teleoperation. In *2018 IEEE International Conference on Robotics and Automation (ICRA)*, pages 1–8. IEEE, 2018.

A. Relabeling play

Algorithm 2 Creating millions of goal image conditioned imitation examples from teleoperated play.

```

1: Input:  $\mathcal{S} = \{(s_{0:t}, a_{0:t})^n\}_n^\infty$ , the unsegmented stream
   of observations and actions recorded during play.
2: Input:  $D_{\text{play}} \leftarrow \{\}$ .
3: Input:  $w_{\text{low}}, w_{\text{high}}$ , bounds on hindsight window size.

4: while True do
5:   # Get next play episode from stream.
6:    $(s_{0:t}, a_{0:t}) \sim \mathcal{S}$ 
7:   for  $w = w_{\text{low}} \dots w_{\text{high}}$  do
8:     for  $i = 0 \dots (t - w)$  do
9:       # Select each  $w$ -sized window.
10:       $\tau = (s_{i:i+w}, a_{i:i+w})$ 
11:      # Treat last observation in window as goal.
12:       $s_g = s_w$ 
13:      Add  $(\tau, s_g)$  to  $D_{\text{play}}$ 
14:    end for
15:  end for
16: end while

```

Algorithm 3 Pairing robot sensor data with natural language instructions.

```

1: Input:  $D_{\text{play}}$ , a relabeled play dataset holding  $(\tau, s_g)$ 
   pairs.
2: Input:  $D_{(\text{play}, \text{lang})} \leftarrow \{\}$ .
3: Input: get_hindsight_instruction(): human overseer,
   providing after-the-fact natural language instructions
   for a given  $\tau$ .
4: Input:  $K$ , number of pairs to generate,  $K \ll |D_{\text{play}}|$ .

5: for  $0 \dots K$  do
6:   # Sample random trajectory from play.
7:    $(\tau, -) \sim D_{\text{play}}$ 
8:   # Ask human for instruction making  $\tau$  optimal.
9:    $l = \text{get\_hindsight\_instruction}(\tau)$ 
10:  Add  $(\tau, l)$  to  $D_{(\text{play}, \text{lang})}$ 
11: end for

```

B. LangLFP Implementation Details

Below we describe the networks we use for perception, natural language understanding, and control—all trained end-to-end as a single neural network to maximize our multicontext imitation objective. We stress that this is only one implementation of possibly many for LangLFP, which is a general high-level framework 1) combining relabeled play, 2) play paired with language, and 3) multicontext imitation.

Layer	Details
Input RGB Image	200 x 200 x 3
Conv2D	32 filters, 8 x 8, stride 4
Conv2D	64 filters, 4 x 4, stride 2
Conv2D	64 filters, 3 x 3, stride 1
Spatial softmax	
Flatten	
Fully connected	512 hidden units, relu
Fully connected	64 output units, linear

Table 3: Hyperparameters for vision network.

B.1. Perception Module

We map raw observations (image and proprioception) to low dimensional perceptual embeddings that are fed to the rest of the network. To do this we use the perception module described in Figure 9. We pass the image through the network described in Table 3, obtaining a 64-dimensional visual embedding. We then concatenate this with the proprioception observation (normalized to zero mean, unit variance using training statistics). This results in a combined perceptual embedding of size 72. This perception module is trained end to end to maximize the final imitation loss. We do no photometric augmentation on the image inputs, but anticipate this may lead to better performance.

B.2. Image goal encoder

g_{enc} takes as input image goal observation O_g and outputs latent goal z . To implement this, we reuse the perception module P_θ , described in Appendix B.1, which maps O_g to s_g . We then pass s_g through a 2 layer 2048 unit ReLU MLP to obtain z .

B.3. Language understanding module

From scratch. For LangLFP, our latent language goal encoder, s_{enc} , is described in Figure 9. It maps raw text to a 32 dimensional embedding in goal space as follows: 1) apply subword tokenization, 2) retrieve learned 8-dim subword embeddings from a lookup table, 3) summarize the sequence of subword embeddings (we considered average pooling and RNN mechanisms for this, choosing average pooling based on validation), and 4) pass the summary through a 2 layer 2048 unit ReLU MLP. Out-of-distribution subwords are initialized as random embeddings at test time.

Transfer learning. For our experiments, we chose Multilingual Universal Sentence Encoder described in (Yang et al., 2019). MUSE is a multitask language architecture trained generic multilingual corpora (e.g. Wikipedia, mined question-answer pair datasets), and has a vocabulary of 200,000 subwords. MUSE maps sentences of any length to a 512-dim vector. We simply treat these embeddings as

Hyperparameter	Value
hardware configuration	8 NVIDIA V100 GPUs
action distribution	discretized logistic, 256 bins per action dimension (Salimans et al., 2017)
optimizer	Adam
learning rate	2e-4
hindsight window low	16
hindsight window high	32
LMP β	0.01
batch size (per GPU)	2048 sequences * padded max length 32 = 65,536 frames
training time	3 days

Table 4: **Training Hyperparameters**

language observations and do not finetune the weights of the model. This vector is fed to a 2 layer 2048 unit ReLU MLP, projecting to latent goal space.

We note there are many choices available for encoding raw text in a semantic pretrained vector space. MUSE showed results immediately and we moved onto different decisions. We look forward to experimenting with different choices of pretrained embedder in the future.

B.4. Control Module

Multicontext LMP. Here we describe “multicontext LMP”: LMP adapted to be able to take either image or language goals. This imitation architecture learns both an abstract visuo-lingual goal space z^g , as well as a plan space z^p capturing the many ways to reach a particular goal. We describe this implementation now in detail.

As a conditional seq2seq VAE, original LMP trains 3 networks. 1) A posterior $q(z^p|\tau)$, mapping from full state-action demonstration τ to a distribution over recognized plans. 2) A learned prior $p(z^p|s_0, s_g)$, mapping from initial state in the demonstration and goal to a distribution over possible plans for reaching the goal. 3) A goal and plan conditioned policy $p(a_t|s_t, s_g, z^p)$, decoding the recognized plan with teacher forcing to reconstruct actions that reach the goal.

To train multicontext LMP, we simply replace the goal conditioning on s_g everywhere with conditioning on z^g , the latent goal output by multicontext encoders $\mathcal{F} = \{g_{\text{enc}}, s_{\text{enc}}\}$. In our experiments, g_{enc} is a 2 layer 2048 unit ReLU MLP, mapping from encoded goal image s_g to a 32 dimensional latent goal embedding. s_{enc} is a subword embedding summarizer described in Section B.3. Unless specified otherwise, the LMP implementation in this paper uses the same hyperparameters and network architecture as in (Lynch et al., 2019). See appendix there for details on the posterior, conditional prior, and decoder architecture, consisting of a RNN, MLP, and RNN respectively.

B.5. Training Details

At each training step, we compute two contextual imitation losses: image goal and language goal. The image goal forward pass is described in Figure 16. The language goal forward pass is described in Figure 17. We share the perception network and LMP networks (posterior, prior, and policy) across both steps. We average minibatch gradients from image goal and language goal passes and we train everything—perception networks, g_{enc} , s_{enc} , posterior, prior, and policy—end-to-end as a single neural network to maximize the combined training objective. We describe all training hyperparameters in Table 4.

C. Environment

We use the same simulated 3D playground environment as in (Lynch et al., 2019), keeping the same observation and action spaces. We define these below for completeness.

C.1. Observation space

We consider two types of experiments: pixel and state experiments. In the pixel experiments, observations consist of (image, proprioception) pairs of 200x200x3 RGB images and 8-DOF internal proprioceptive state. Proprioceptive state consists of 3D cartesian position and 3D euler orientation of the end effector, as well as 2 gripper angles. In the state experiments, observations consist of the 8D proprioceptive state, the position and euler angle orientation of a movable block, and a continuous 1-d sensor describing: door open amount, drawer open amount, red button pushed amount, blue button pushed amount, green button pushed amount. In both experiments, the agent additionally observes the raw string value of a natural language text channel at each timestep.

C.2. Action space

We use the same action space as (Lynch et al., 2019): 8-DOF cartesian position, euler, and gripper angle of the end effector. Similarly, during training we quantize each action

element into 256 bins. All stochastic policy outputs are represented as discretized logistic distributions over quantization bins (Salimans et al., 2017).

D. Datasets

D.1. Play dataset

We use the same play logs collected in (Lynch et al., 2019) as the basis for all relabeled goal image conditioned learning. This consists of ~ 7 h of play relabeled in to D_{play} : ~ 10 M short-shorizon windows, each spanning 1-2 seconds.

D.2. (Play, language) dataset

We pair 10K windows from D_{play} with natural language hindsight instructions using the interface shown in Fig. 10 to obtain $D_{(\text{play}, \text{lang})}$. See real examples below in Table 5. Note the language collected has significant diversity in length and content.

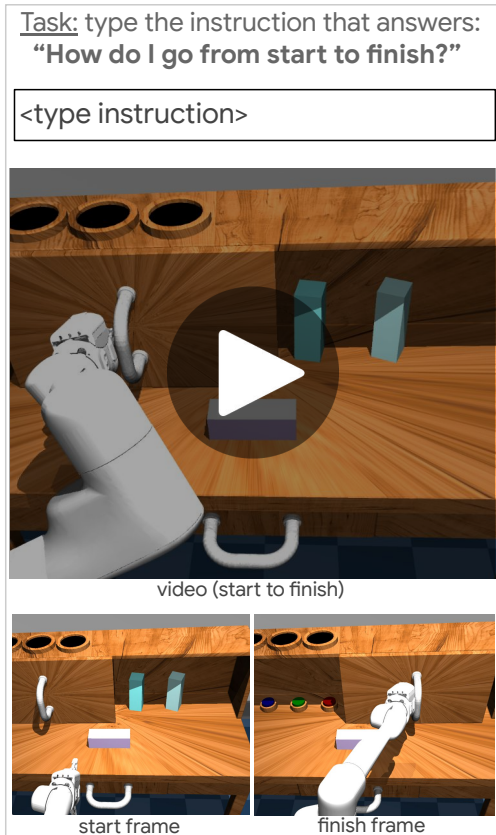


Figure 10: A schematic rendering of our hindsight language collection tool.

Fig. 10 demonstrates how hindsight instructions are collected. Overseers are presented with a webpage that contains a looping video clip of 1 to 2 seconds of play, along with the first and the last frames of that video, to help them

identify the beginning and the end of the clip if necessary. Overseers are asked to type in a text box the sentence that best answers the question "How do I go from start to finish?". Several considerations can go into the design of this interface. First, we can ask overseers to type in multiple instructions that are as different from each other as possible, to increase generalization and diversity of the language dataset. After experimenting with one or multiple text boxes, we opted for using only one, while asking users to write as diverse sentences as possible throughout the collection process. A disadvantage of having multiple boxes is that it can sometimes be challenging to come up with diverse sentences when the observed action is very simple. It also leads to less video-language pairs for the same budget. Thus we decided one sentence per video was most beneficial in our case. Another collection consideration is the level of details in a sentence. For example, for a generalist robot application, it seems "open the drawer" is a more likely use case than "move your hand 10 cm to the right above the drawer handle, then grasp the drawer handle, then pull on the drawer handle". Similarly, an instruction geared toward a function such as "open the drawer" is more likely useful than one detached from it function, e.g. "put your fingers around the drawer handle, pull your hand back". Finally, given the temporal horizon of our video clips, multiple things can be happening within one clip. How many events should be described? For example it might be important to describe multiple motions such as "close the drawer then reach for the object". With all these observations in mind, we instructed the overseers to only describe the main actions, while asking themselves: which instructions would I give to another human being so that they could produce a similar video if they were in that scene?.

D.3. (Demo, language) dataset

To define $D_{(\text{demo}, \text{lang})}$, we pair each of the 100 demonstrations of the 18 evaluation tasks from (Lynch et al., 2019) with hindsight instructions using the same process as in 4.1. We similarly pair the 20 test time demonstrations of each of the 18 tasks. See examples for each of the tasks in Table 6. 74.3% of the natural language instructions in the test dataset appear at least once in D_{play} . 85.08% of the instructions in $D_{(\text{play}, \text{lang})}$ never appear in the test set.

D.4. Restricted play dataset

For a controlled comparison between LangLFP and LangBC, we train on a play dataset restricted to the same size as the aggregate multitask demonstration dataset (~ 1.5 h). This was obtained by randomly subsampling the original play logs ~ 7 h to ~ 1.5 h before relabeling.

“grasp the object from the drawer and drop it on the table”
 “pick the object and then lift it up.”
 “pull the drawer.”
 “drag the object into the drawer”
 “drop the object, and again pickup the object high”
 “close the drawer”
 “do nothing.”
 “move your hand to the right”
 “push the door to the right.”
 “reach for the green button”
 “slightly close your hand.”
 “go grasp the door handle”
 “close the drawer”
 “drop the object and push it inside the shelf”
 “grasp the block and drop it on top of the table”
 “place the block on top of the table”
 “rotate the block 90 degrees to the right”
 “move the cabinet door to the right and then release your fingers.”
 “open the drawer”
 “slightly close the drawer, then drag it a little bit , close it and then let go”
 “reach for the object.”
 “press the red button and then release it”
 “move your hand towards the door handle”
 “drop the object”
 “slightly pull the drawer and then reach for its handle.”
 “drop the object in the drawer”
 “release the block and move your hand upwards.”
 “drop the object on the table and reach for the door handle”
 “push the object into to the drawer”
 “slightly move the door to the right, then drop the object and again turn the object to the left”
 “slowly move the door to the left”

Table 5: Randomly sampled examples from the training set of hindsight instructions paired with play. As hindsight instruction pairing sits on top of play, the language we collect is similarly not constrained by predefined tasks, and instead covers both specific functional behaviors and general, non task-specific behaviors.

Task	Natural language instructions
open sliding door	“move the door all the way to the right” “slide the door to the right” “move the sliding door all the way to the right and let go”
close sliding door	“Grasp the door handle, then slide the door to the left” “move the door all the way to the left”
open drawer	“open the cabinet drawer” “open the drawer and let go”
close drawer	“close the drawer and let go” “close the drawer”
grasp flat	“Pick up the block” “grasp the object and lift it up” “grasp the object and move your hand up”
grasp lift	“Pick up the object from the drawer and drop it on the table.” “hold the block and place it on top of the table”
grasp upright	“Pick the object and lift it up” “grasp the object and lift”
knock	“push the block forward” “push the object towards the door”
pull out shelf	“Drag the block from the shelf towards the drawer” “pick up the object from the shelf and drop it on the table”
put in shelf	“grasp the object and place it inside the cabinet shelf” “Pick the object, move it into the shelf and then drop it.”
push red	“go press the red button” “Press the red button”
push green	“press the green button” “push the green button”
push blue	“push the blue button” “press down on the blue button.”
rotate left	“Pick up the object, rotate it 90 degrees to the left and drop it on the table” “rotate the object 90 degrees to the left”
rotate right	“turn the object to the right” “rotate the block 90 degrees to the right”
sweep	“roll the object into the drawer” “drag the block into the drawer”
sweep left	“Roll the block to the left” “close your fingers and roll the object to the left”
sweep right	“roll the object to the right” “Push the block to the right.”

Table 6: Example natural language instructions used to specify the 18 test-time visual manipulation tasks.

E. Models

Below we describe our various baselines and their training sources. Note that for a controlled comparison, all methods are trained using the exact same architecture described in Section B, differing only on the source of data.

Method	Training Data
LangBC	$D_{(\text{demo}, \text{lang})}$
LfP (goal image)	D_{play}
LangLfP Restricted	restricted $D_{\text{play}}, D_{(\text{play}, \text{lang})}$
LangLfP (ours)	$D_{\text{play}}, D_{(\text{play}, \text{lang})}$
TransferLangLfP (ours)	$D_{\text{play}}, D_{(\text{play}, \text{lang})}$

Table 7: Methods and their training data sources. All baselines are trained to maximize the same generalized contextual imitation objective MCIL.

F. Long Horizon Evaluation

Task construction. We construct long-horizon evaluations by considering transitions between the 18 subtasks defined in (Lynch et al., 2019). These span multiple diverse families, e.g. opening and closing doors and drawers, pressing buttons, picking and placing a movable block, etc. For example, one of the 925 Chain-4 tasks may be “open_sliding, push_blue, open_drawer, sweep”. We exclude as invalid any transitions that would result in instructions that would have necessarily already been satisfied, e.g. “open_drawer, press_red, open_drawer”. To allow natural language conditioning we pair 20 test demonstrations of each subtask with human instructions using the same process as in Section 4.1 (example sentences in Table 6).

Eval walkthrough. The long horizon evaluation happens as follows. For each of the N-stage tasks in a given benchmark, we start by resetting the scene to a neutral state. This is discussed more in the next section. Next, we sample a natural language instruction for each task in the N-stage sequence from a test set. Next, for each subtask in a row, we condition the agent on the current subtask instruction and rollout the policy. If at any timestep the agent successfully completes the current subtask (according to the environment-defined reward), we transition to the next subtask in the sequence (after a half second delay). This attempts to mimic the qualitative scenario where a human provides one instruction after another, queuing up the next instruction, then entering it only once the human has deemed the current subtask solved. If the agent does not complete a given subtask in 8 seconds, the entire episode ends in a timeout. We score each multi-stage rollout by the percent of subtasks completed, averaging over all multi-stage tasks in the benchmark to arrive at the final N-stage number.

Neutrality in multitask evaluation. When evaluating any context conditioned policy (goal-image, task id, natural lan-

guage, etc.), a natural question that arises is: how much is the policy relying on the context to infer and solve the task? Previously in Lynch et al. (2019), evaluation began by resetting the simulator to the first state of a test demonstration, ensuring that the commanded task was valid. We find that under this reset scheme, the initial pose of the agent can in some cases become correlated with the task, e.g. arm nearby the drawer for a drawer opening task. This is problematic, as it potentially reveals task information to the policy through the *initial state*, rather than the context.

In this work, we instead reset the arm to a fixed neutral position at the beginning of every test episode. This “neutral” initialization scheme is used to run all evaluations in this paper. We note this is a fairer, but significantly more difficult benchmark. Neutral initialization breaks correlation between initial state and task, forcing the agent to rely entirely on language to infer and solve the task. For completeness, we present evaluation curves for both LangLfP and LangBC under this and the prior possibly “correlated” initialization scheme in Figure 11. We see that when LangBC is allowed to start from the exact first state of a demonstration (a rigid real world assumption), it does well on the first task, but fails to transition to the other tasks, with performance degrading quickly after the first instruction (Chain-2, Chain-3, Chain-4). Play-trained LangLfP on the other hand, is far more robust to change in starting position, experiencing only a minor degradation in performance when switching from the correlated initialization to neutral.

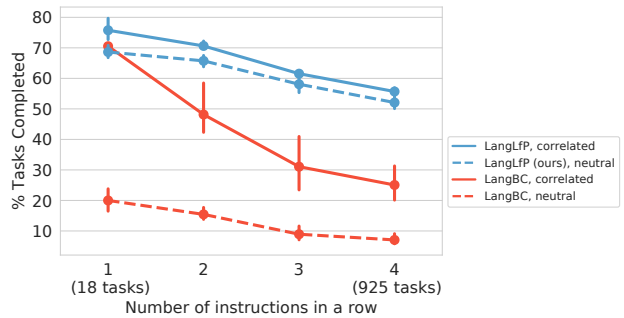


Figure 11: **Training on relabeled play leads to robustness.** Models trained on relabeled play (LangLfP) are robust to a fixed neutral starting position during multitask evaluation, models trained on conventional predefined demonstrations (LangBC) are not.

G. Qualitative Examples

G.1. Composing new tasks with language

In this section, we show some difficult tasks that LangLfP can achieve by having the operator breaking them down into multiple instructions. These tasks are achieved in zero shot and are not included in the standard 18-task benchmark.

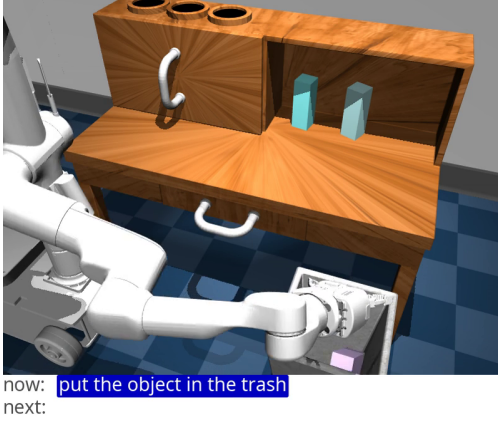


Figure 12: **Putting the object in the trash:** An operator is able to put the object in the trash by breaking down the task into 2 smaller subtasks with the following sentences; 1) "pick up the object" 2) "put the object in the trash"

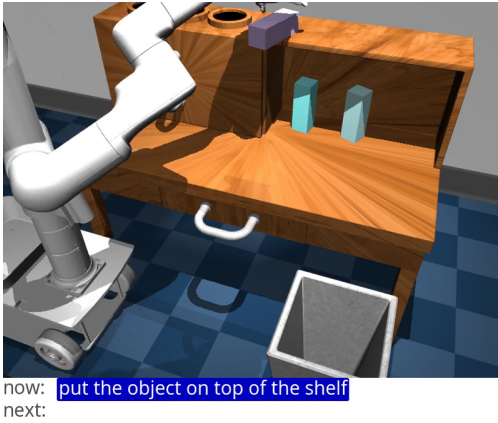


Figure 13: **Putting the object on top of the shelf:** An operator is able to put the object in the trash by breaking down the task into 2 smaller subtasks with the following sentences; 1) "pick up the object" 2) "put the object on top of the shelf"

G.2. The Operator Can Help the Robot

In this section, we show an example of the human operator adapting its instructions if the robot gets stuck, and adding extra sub-steps to get out of trouble and fix the situation in order to achieve the initial instruction. In Fig. 14, the robot gets its end-effector stuck against the door on the way to pressing the red button. The operator then changing the command to move back, then opening the door more to the right so that it has better access to the red button, then pressing the red button.

H. Ablation: How much language is necessary?

We study how the performance of LangLfp scales with the number of collected language pairs. Figure 15 compares

models trained from pixel inputs to models trained from state inputs as we sweep the amount of collected language pairs by factors of 2. Interestingly, for models trained from states, doubling the size of the language dataset from 5k to 10k has marginal benefit on performance. Models trained from pixels, on the other hand, have yet to converge and may benefit from even larger datasets. This suggests that the role of larger language pair datasets is primarily to address the complicated perceptual grounding problem.

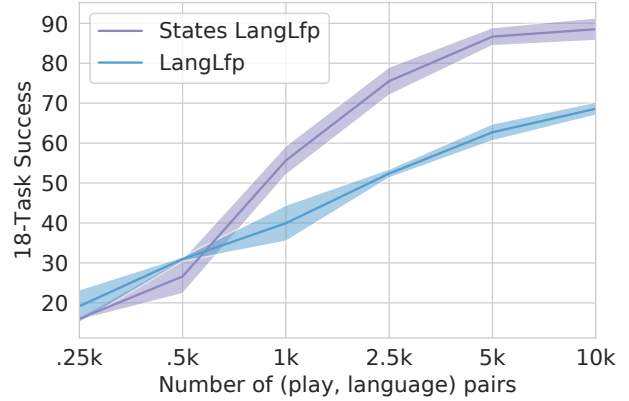
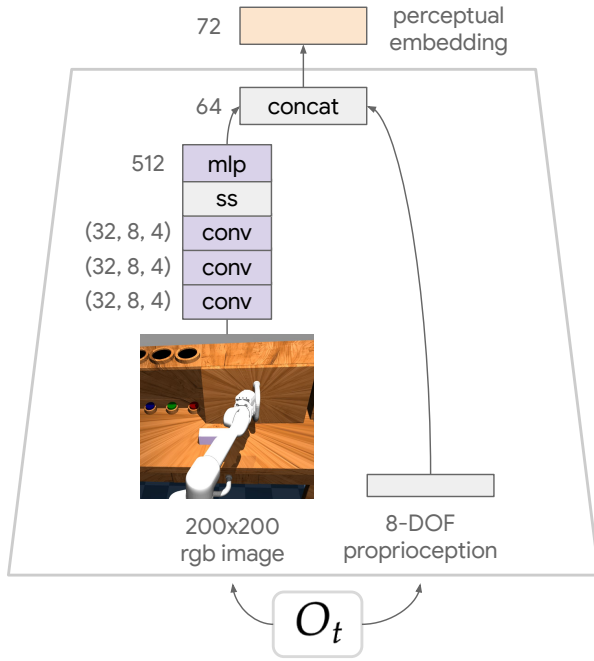


Figure 15: **18-task success vs amount of human language pairs**

Perception



Language goal encoder

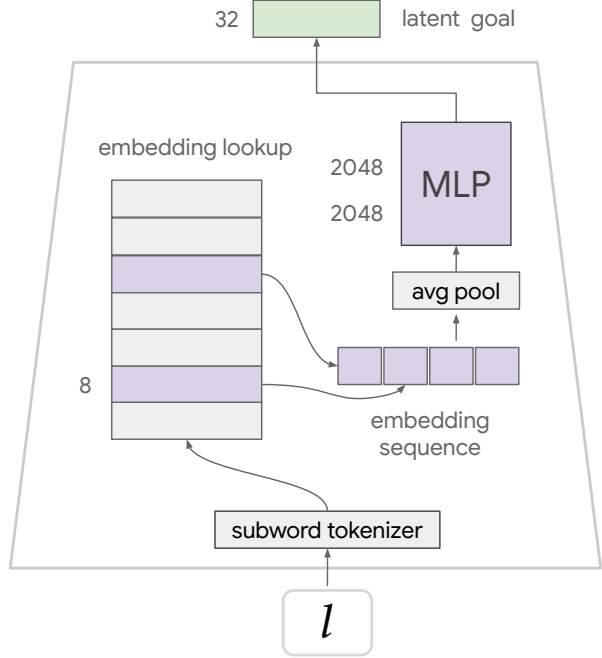
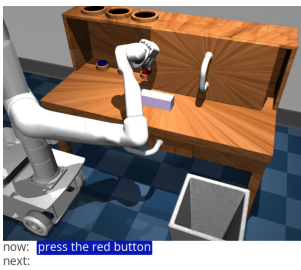


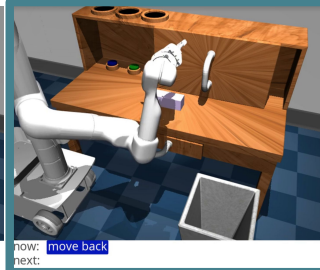
Figure 9: Perception and language embedder modules

agent gets stuck

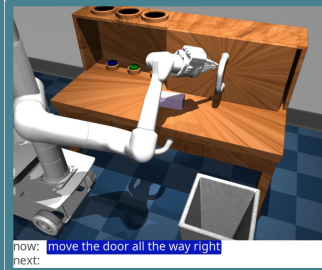


“press the red button”

human assists with language



“move back”



“move the door all the way right”

agent solves task



“press the red button”

Figure 14: **Getting out of trouble and adding steps to achieve a task:** from top to bottom we see how the operator adapted the instructions. The operator initially asks the robot to “press the red button”, but the door is not fully moved to the right so the robot end-effector gets stuck against it. The operator then asks the robot to “move back” and “move the door all the way right” so that it does not get stuck again. Then finally, the operator repeats “press the red button” which the robot can now more easily achieve.

Multicontext LMP: goal image

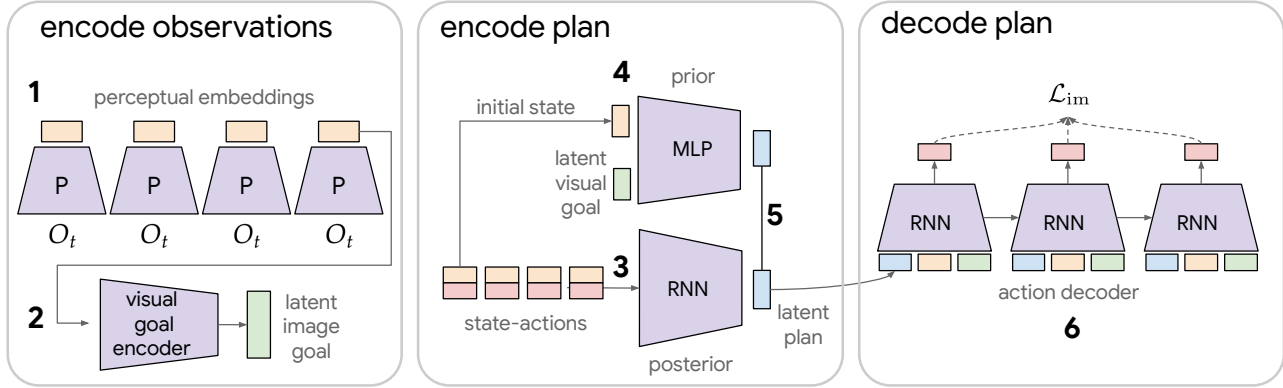


Figure 16: **Latent image goal LMP**: This image goal conditioned forward pass of multicontext LMP. 1) Map sequence of raw observations O_t to perceptual embeddings (see Figure 9). 2) Map image goal to latent goal space. 3) Map full state-action sequence to recognized plan through posterior. 4) Map initial state and latent goal through prior network to distribution over plans for achieving goal. 5) Minimize KL divergence between posterior and prior. 6) Compute maximum likelihood action reconstruction loss by decoding plan into actions with teacher forcing. Each action prediction is conditioned on current perceptual embedding, latent image goal, and latent plan. Note perception net, posterior, prior, and policy are shared with language goal forward pass.

Multicontext LMP: language

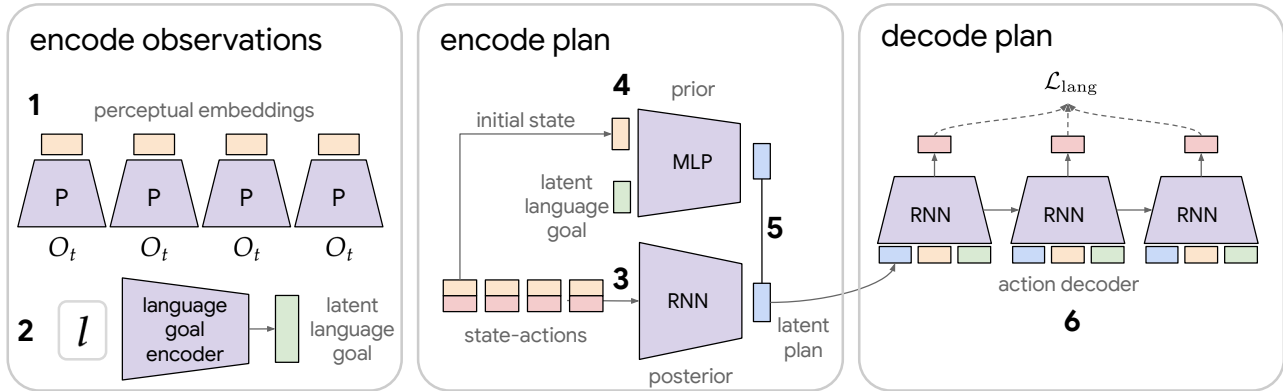


Figure 17: **Latent language goal LMP**: This describes the language goal conditioned forward pass of multicontext LMP. 1) Map sequence of raw observations O_t to perceptual embeddings (see Figure 9). 2) Map language observation to latent goal space. 3) Map full state-action sequence to recognized plan through posterior. 4) Map initial state and latent goal through prior network to distribution over plans for achieving goal. 5) Minimize KL divergence between posterior and prior. 6) Compute maximum likelihood action reconstruction loss by decoding plan into actions with teacher forcing. Each action prediction is conditioned on current perceptual embedding, latent language goal, and latent plan. Note perception net, posterior, prior, and policy are shared with image goal LMP.